



THE UNIVERSITY *of* EDINBURGH

## Edinburgh Research Explorer

### Multiple circadian clock outputs regulate diel turnover of carbon and nitrogen reserves

**Citation for published version:**

Flis, A, Mengin, V, Ivakov, AA, Mugford, ST, Hubberten, H-M, Encke, B, Krohn, N, Höhne, M, Feil, R, Hoefgen, R, Lunn, JE, Millar, AJ, Smith, AM, Sulpice, R & Stitt, M 2019, 'Multiple circadian clock outputs regulate diel turnover of carbon and nitrogen reserves', *Plant, Cell and Environment*, vol. 42, no. 2, pp. 549-573. <https://doi.org/10.1111/pce.13440>

**Digital Object Identifier (DOI):**

[10.1111/pce.13440](https://doi.org/10.1111/pce.13440)

**Link:**

[Link to publication record in Edinburgh Research Explorer](#)

**Document Version:**

Peer reviewed version

**Published In:**

Plant, Cell and Environment

**Publisher Rights Statement:**

This article has been accepted for publication and undergone full peer review but has not been through the copyediting, typesetting, pagination and proofreading process which may lead to differences between this version and the Version of Record. Please cite this article as doi: 10.1111/pce.13440

**General rights**

Copyright for the publications made accessible via the Edinburgh Research Explorer is retained by the author(s) and / or other copyright owners and it is a condition of accessing these publications that users recognise and abide by the legal requirements associated with these rights.

**Take down policy**

The University of Edinburgh has made every reasonable effort to ensure that Edinburgh Research Explorer content complies with UK legislation. If you believe that the public display of this file breaches copyright please contact [openaccess@ed.ac.uk](mailto:openaccess@ed.ac.uk) providing details, and we will remove access to the work immediately and investigate your claim.



Running title: Metabolism in five circadian clock mutants

# Multiple circadian clock outputs regulate diel turnover of carbon and nitrogen reserves

Anna Flis<sup>1,2\*</sup>, Virginie Mengin<sup>1\*</sup>, Alexander A. Ivakov<sup>1,2</sup>, Sam T. Mugford<sup>5</sup>, Hans-Michael Hubberten<sup>1</sup>, Beatrice Encke<sup>1</sup>, Nicole Krohn<sup>1</sup>, Melanie Höhne<sup>1</sup>, Regina Feil<sup>1</sup>, Rainer Hoefgen<sup>1</sup>, John E. Lunn<sup>1</sup>, Andrew J. Millar<sup>4</sup>, Alison M. Smith<sup>5</sup>, Ronan Sulpice<sup>1,3</sup> and Mark Stitt<sup>1</sup>.

<sup>1</sup> Max Planck Institute for Molecular Plant Physiology, 14476 Potsdam-Golm, Germany

<sup>2</sup> Present Address: ARC Centre of Excellence for Translational Photosynthesis, Research School of Biology, Australian National University, Canberra, ACT, 2601, Australia

<sup>3</sup> Present Address: NUIG, Plant Systems Biology Lab, Plant and AgriBiosciences Research Centre, Ryan Institute, Galway, Ireland

<sup>4</sup> SynthSys and School of Biological Sciences, C.H. Waddington Building, University of Edinburgh, Edinburgh EH9 3BF, UK

<sup>5</sup> John Innes Centre, Norwich Research Park, Norwich NR4 7UH, UK

\* Denotes equal contribution

Corresponding author: Mark Stitt, [mstitt@mpimp-golm.mpg.de](mailto:mstitt@mpimp-golm.mpg.de)

**ORCIDs:** A.F. 0000-0002-9142-1606; V.M. 0000-0002-4958-4209; A.A.I. 0000-0003-4091-1135; S.T.M. 0000-0002-8537-5578; R.F. 0000-0002-9936-1337; R.H. 0000-0001-8590-9800; J.E.L. 0000-0001-8533-3004; A.J.M. 0000-0003-1756-3654; A.M.S. 0000-0001-6927-9650; R.S. 0000-0002-6113-9570; M.S. 0000-0002-4900-1763

## Word count

Abstract	199
Introduction	1623
Materials and Methods	2273
Results	5769
Discussion	4871

This article has been accepted for publication and undergone full peer review but has not been through the copyediting, typesetting, pagination and proofreading process which may lead to differences between this version and the Version of Record. Please cite this article as doi: 10.1111/pce.13440

## Abstract

Plants accumulate reserves in the daytime to support growth at night. Circadian regulation of diel reserve turnover was investigated by profiling starch, sugars, glucose 6-phosphate, organic acids and amino acids during a light-dark cycle and after transfer to continuous light in *Arabidopsis* wild-types and in mutants lacking dawn (*lhy cca1*), morning (*prp7 prp9*), dusk (*toc1, gi*) or evening (*elf3*) clock components. The metabolite time-series were integrated with published time-series for circadian clock transcripts to identify circadian outputs that regulate central metabolism. i) Starch accumulation was slower in *elf3* and *prp7 prp9*. It is proposed that *ELF3* positively regulates starch accumulation. ii) Reducing sugars were high early in the T-cycle in *elf3*, revealing that *ELF3* negatively regulates sucrose recycling. iii) The pattern of starch mobilization was modified in all five mutants. A model is proposed in which dawn and dusk/evening components interact to pace degradation to anticipated dawn. iv) An endogenous oscillation of glucose 6-phosphate revealed that the clock buffers metabolism against the large influx of carbon from photosynthesis. v) Low levels of organic and amino acids in *lhy cca1* and high levels in *prp7 prp9* provide evidence that the dawn components positively regulate the accumulation of amino acid reserves.

## Keywords

*Arabidopsis*, circadian clock, nitrogen metabolism, sugar, starch

## Summary statement - PCE-18-0607 (Flis *et al.*)

Plants accumulate reserves in the light period to support metabolism, maintenance and growth during the night. We have performed time-resolved measurement of starch and other central metabolites in five circadian clock mutants in light-dark cycles and after releasing them in continuous light. The metabolite time-series were integrated with published time-series for circadian clock transcripts to identify circadian outputs that regulate diel metabolism. Clock outputs are identified that regulate starch synthesis, starch degradation and the accumulation of organic acids and amino acids.

## Introduction

Circadian clocks act as internal time-keepers to generate endogenous rhythms with a period of about 24 h (Dong & Golden 2008; Zhang & Kay 2010). They are entrained by external inputs that synchronize them with the external light-dark cycle, allowing them to operate as reliable timekeepers in a wide range of environmental conditions (Johnson *et al.* 2003; Millar 2004; Dodd *et al.* 2005; Greenham & McClung 2015). In plants, light is both a signal and the energy source that drives photosynthesis, metabolism and growth. Optimal growth in light-dark cycles requires accumulation of carbon (C) and nitrogen (N) reserves in the light and their mobilization to support metabolism and growth in darkness (Smith & Stitt 2007). One function of the plant circadian clock is to coordinate metabolism, reserve turnover and growth with the daily cycle of light and darkness (Millar 2004; Dodd *et al.* 2005; Zhang & Kay 2010; Graf & Smith 2011; Farré & Weise 2012; Seo & Mas 2014; Greenham & McClung 2015).

The Arabidopsis circadian clock can be schematized as an interconnected network consisting of a four-loop structure of ‘dawn’, ‘day’, ‘dusk’ and ‘evening’ components coupled around a repressilator (Nakamichi 2011; Pokhilko *et al.* 2012; Carré & Veflingstad 2013; Fogelmark & Troein 2014). In addition, *REVEILLE* (*RVE*) family members promote expression of many circadian clock components (Hsu *et al.* 2013; Fogelmark & Troein 2014). At the start of the 24 h cycle there is high expression of the dawn components (*LHY*, *CCA1*), followed by the day (*PRR9*, *PRR7*), dusk (*PRR5*, *TOC1*) and Evening Complex (EC; *ELF3*, *ELF4*, *LUX*) components. As the 24-h cycle progresses, expression of day, dusk and EC genes decays or self-represses, relieving the repression of *LHY* and *CCA1* transcripts which rise to a peak at the next dawn. Light signaling influences the circadian clock at multiple sites (Edwards *et al.* 2010; Kinmonth-Schultz *et al.* 2013; Staiger *et al.* 2013; Seo & Mas 2014). The Arabidopsis circadian clock is largely dawn-dominant because light positively regulates the dawn and day components, whilst dark-instability of many dusk and evening complex components accelerates progression of the circadian clock cycle after darkening (Edwards *et al.* 2010; Seaton *et al.* 2015; Song *et al.* 2015; Flis *et al.* 2016).

Starch is the major transient C reserve in Arabidopsis and many other plants (Smith & Stitt 2007). Starchless mutants or mutants with defects in starch degradation can grow in continuous light or long photoperiods, but their growth is severely impaired in intermediate or short photoperiods (Caspar *et al.* 1985; Gibon *et al.* 2004a). Absence or premature exhaustion of starch at night results in inhibition of protein and cell wall synthesis, wasteful

catabolism of protein and other cellular components, and an inhibition of growth that lasts for several hours after re-illumination (Gibon *et al.* 2004a; Usadel *et al.* 2008; Yazdanbakhsh *et al.* 2011; Izumi *et al.* 2013; Pal *et al.* 2013; Yadav *et al.* 2014; Apelt *et al.* 2015; Ishihara *et al.* 2015).

Many plants including *Arabidopsis* increase the rate of starch accumulation and decrease the rate of mobilization in short photoperiods, allowing them to avoid premature exhaustion of starch before dawn (reviewed in Smith & Stitt 2007, see also Gibon *et al.* 2009; Sulpice *et al.* 2014). Whilst it is unclear if the circadian clock directly regulates starch accumulation (Mugford *et al.* 2014), it undoubtedly plays a key role at night. Starch mobilization is paced such that starch is almost but not completely exhausted at dawn, as anticipated by the circadian clock (Graf & Smith 2011; Scialdone *et al.* 2013; Scialdone & Howard 2015). Wild-type plants pace mobilization to about 24 h after the previous dawn, with the result that starch is incompletely exhausted in a T-17 cycle and is prematurely exhausted in a T-28 cycle (Graf *et al.* 2010). Starch is exhausted prematurely in the short period *lhy cca1* mutant (Graf *et al.* 2010; Scialdone *et al.* 2013) resulting in an inhibition of growth before dawn that can be prevented by growing the mutant in a short T-cycle (Graf *et al.* 2010; Apelt *et al.* 2017) or by providing exogenous sugar (Yazdanbakhsh *et al.* 2011). This underlines the importance of correctly timing starch mobilization. Circadian pacing of starch mobilization allows plants to cope with rapid environmental fluctuations including decreased irradiation during the light period, an interruption of the night or sudden changes in night temperature (Lu *et al.* 2005; Graf *et al.* 2010; Pyl *et al.* 2012; Scialdone *et al.* 2013; Pilkington *et al.* 2014).

Scialdone *et al.* (2013) proposed that plants set an appropriate rate of starch mobilization at night by arithmetic division of the starch content by the remaining time to dawn. However, the molecular mechanisms by which the circadian clock provides information about time to dawn and starch content is measured are unknown (Scialdone *et al.* 2013; Seaton *et al.* 2014). The biochemical mechanisms that directly regulate the rate of degradation are also unknown, although it is suspected that they involve modulation of a cycle of glucan phosphorylation and dephosphorylation that renders the surface of the starch granule susceptible to  $\beta$ -amylolytic attack (Scialdone *et al.* 2013).

Plants also build up nitrogen reserves to support protein synthesis and growth at night. Rapid assimilation of nitrate and ammonium in the light leads to accumulation of amino acids (Scheible *et al.* 2000; Urbanczyk-Wochniak *et al.* 2005; Fritz *et al.* 2006a,b; Piques *et al.*

2009; Pal *et al.* 2013; Sulpice *et al.* 2014a). As nitrate and ammonium assimilation account for half the total cost of protein synthesis (Penning De Vries 1975; Amthor 2000), accumulation of amino acids in the light allows a substantial reduction of growth costs in the following night.

Diel amino acid turnover is less intensively researched than starch turnover. Nevertheless, there is suggestive evidence that N metabolism is subject to circadian regulation. Nitrate reductase (NR) protein and activity show strong diel changes due to regulation at the level of transcription, translation, protein stability and post-transcriptional modification (Vincentz *et al.* 1993; Scheible *et al.* 1997; Campbell 1999; Stitt *et al.* 2002). Whilst this is partly due to regulation by light and C, NR expression is also under circadian regulation (Deng *et al.* 1991; Pilgrim *et al.* 1993; Lillo *et al.* 2001). The finding that many amino acids peak after subjective dusk in continuous light points to circadian regulation of their turnover (Espinoza *et al.* 2010). Plants with altered clocks due to loss of *prp9*, *prp7* and *prp5* or over-expression of *CCA1* have elevated levels of many amino acids in light-dark cycles, which may be attributable to higher tricarboxylic acid cycle (TCA) activity and higher levels of organic acids (Fukushima *et al.* 2009). However, it is difficult to conclude if this metabolic phenotype is a direct or indirect effect of the profoundly altered clock function in these plants. Independent support for circadian regulation of N metabolism was provided by Gutierrez *et al.* (2008) who identified *CCA1* as a hub in a transcriptional network that includes genes in central N metabolism. Further evidence for a link between the clock and N-metabolism comes from studies of the *tic* mutant (deficient in *TIME FOR COFFEE*, *TIC*). *TIC* is involved in resetting the circadian clock around dawn. Its loss leads to modified levels of many amino acids (Sanchez-Villarreal *et al.* 2013), and also affects starch turnover, C-sensing, stress responses and development (Hall *et al.* 2003; Ding *et al.* 2007; Sanchez-Villarreal *et al.* 2013).

Plants also accumulate organic acids in the light (Chia *et al.* 2000; Scheible *et al.* 2000; Urbanczyk-Wochniak *et al.* 2005; Sulpice *et al.* 2014b). Organic acids provide a substrate for respiratory metabolism at night (Fahnenstich *et al.* 2007; Lehmann *et al.* 2015). Furthermore, organic acid metabolism is intertwined with N metabolism. Organic acids act as counter-anions for nitrate (Raven 1986; Britto & Kronzucker 2005) and N-acceptors during amino acid synthesis (Stitt & Krapp 1999; Coruzzi & Zhou 2001; Stitt *et al.* 2002; Novitskaya *et al.* 2002; Miller *et al.* 2007; Nunes-Nesi *et al.* 2010). The *prp5 prp7 prp9* triple mutant, *CCA1*

overexpressing lines and the *tic* mutant showed altered levels of organic acids compared to wild-type plants (Fukushima *et al.* 2009; Sanchez-Villarreal *et al.* 2013).

The core circadian clock is highly integrated, with changes in expression of one component strongly modifying the operation of other components (Pokhilko *et al.* 2012; Fogelmark & Troein 2014). This makes it difficult to distinguish between direct and indirect effects when individual mutants are studied. Furthermore, although transcripts for proteins involved in photosynthesis, sucrose and starch metabolism and nitrogen metabolism often exhibit circadian rhythms (Harmer *et al.* 2000, 2001; Smith *et al.* 2004; Michael *et al.* 2008; Usadel *et al.* 2008; Harmer 2009; Farré & Weise 2012), these rarely lead to significant diel changes in the abundance of the encoded proteins (Gibon *et al.* 2004b, 2006; Baerenfaller *et al.* 2012; Stitt & Gibon 2014; Skeffington *et al.* 2014; Dodd *et al.* 2015; Seaton *et al.* 2018). This underlines the need for studies of emergent metabolic responses that integrate circadian outputs, irrespective of whether the outputs act transcriptionally, post-transcriptionally or post-translationally.

We have performed time-resolved profiling of starch, sugars, glucose 6-phosphate (Glc6P), organic acids and amino acids during vegetative growth in carbon-limiting conditions and after transfer to continuous light in five mutants affected in dawn, morning, dusk or evening components of the circadian clock. The resulting metabolite time-series data were integrated with published time-series for circadian clock transcript abundance in the same plant material (Flis *et al.* 2015). Our aims were to further test the idea that starch degradation at night is regulated by an arithmetic division mechanism, to ask whether the circadian clock also regulates starch synthesis and the accumulation of organic acids and amino acids in the light, and to ask which circadian clock components are involved in these responses.

## Materials and Methods

**Plant material and growth.** The experiments (summarized in Fig. 1A) used Col-0 and Ws-2 wild-types, and the circadian clock mutants *prp7-3 prp9-1* (*prp7 prp9*), *toc1-101* (*toc1*), *gi-201* (*gi*) (Col-0 background) and *lhy-21 cca1-11* (*lhy cca1*) and *elf3-4* (*elf3*) (Ws-2 background). Plants were grown in a 12 h photoperiod ( $160 \mu\text{mol m}^{-2} \text{s}^{-1}$ , 21°C in light, 19°C in dark). The same material was previously used to analyze gene expression (Flis *et al.*, 2015).



Three separate experiments were performed with Col-0 and Ws-2 wild-type and *prp7 prp9*, *toc1*, *gi* and *lhy cca1*, all at 21 days after sowing (DAS21). i) Starting just before dawn (ZT0; ZT: Zeitgeber, time from the previous dawn), samples were taken at 2 h intervals during a complete light-dark cycle (LD). ii) Plants were transferred to continuous light at dusk (ZT12) and sampled at 2 h intervals over a total of 48 h, starting at the dawn before transfer (LLLL). iii) Plants were transferred to constant darkness just before dawn (ZT24) and sampled at 2 h intervals for the next 24 h (DD). Two samples were collected at each sampling time, with 5-10 rosettes per sample (higher number for the smaller *lhy cca1* and *prp7 prp9* mutants). Two experiments were performed with Ws-2 and *elf3*, harvesting on DAS13 because *elf3* is early flowering (Zagotta *et al.* 1992). i) Samples were taken at 2 h intervals starting just before dawn, during the 24 h light-dark cycle and for a further 12 h extension of the night (LDD), and some plants were left in the light at the end of the light period and sampled for another 12 h of extended light (LL) with 3-4 samples per time point (each 20-50 plants). ii) Samples were taken at 2 h intervals through a 24 h light-dark cycle (LD), with two samples per time point (each 30-60 plants, higher for the smaller *elf3* mutant).

To investigate how starch mobilization responds to a sudden early dusk, *prp7 prp9*, *toc1*, *lhy cca1* and Col-0 and Ws-2 wild-types were grown as in Mugford *et al.* (2014). On DAS21 some plants were darkened at ZT8 (Col-0, *prp7 prp9* and *toc1*) or ZT9 (Ws-2, *lhy cca1*). Samples were taken at dawn and throughout the night (6-10 replicates, each one plant). *elf3* was grown as in Flis *et al.* (2015), and on DAS13 some plants were darkened at ZT8; samples were taken at 2 h intervals (3-4 replicates, each 20-50 plants).

Rosettes were harvested into liquid nitrogen within 10-40 sec, stored at -80°C, homogenized using a Ball-Mill (Retsch GmbH, Haan, Germany) and sub-aliquoted in liquid nitrogen.

**Metabolite assays.** Chemicals were purchased as in Gibon *et al.* (2004b). Protein was assayed as in Bradford (1976). Ethanolic extracts of 20 mg frozen plant material were prepared and starch, glucose, fructose, sucrose and total amino acids were determined as in Cross *et al.* (2006) and malate and fumarate as in Nunes-Nesi *et al.* (2007). Assays were performed in 96-well microplates using a Janus pipetting robot (Perkin Elmer, Wellesley, MA, USA). Absorbance was determined using Synergy, ELx800 or ELx808 microplate readers (Bio-Tek, Bad Friedrichshall, Germany). For all the assays, two technical replicates were determined per biological replicate. Phosphorylated intermediates and organic acids were measured by liquid chromatography linked to tandem mass spectrometry (LC-MS/MS)



(Lunn *et al.* 2006) modified as in Figueroa *et al.* (2016). Individual amino acids were measured by high pressure liquid chromatography (HPLC) with pre-column derivation with *O*-phthalaldehyde and fluorescence detection (Watanabe *et al.* 2013).

**Whole rosette photosynthesis and respiration** were measured using a LI-COR portable photosynthesis system LI-6400XT with the Whole Plant Arabidopsis chamber and the RGB LED light source (LI-COR Biosciences, Lincoln, NE, USA). To exclude soil respiration, the soil was covered with plastic film (plants grew through small holes) and the chamber operated at slight over-pressure by restricting exhaust air flow, facilitating air flow through the soil by pin-sized holes in the pot wall. CO<sub>2</sub> concentration was adjusted to 400 ppm using the built-in LI-6400XT CO<sub>2</sub> controller. Relative humidity was around 60% and leaf temperature 20°C. Photosynthesis (*A*) was measured at growth irradiance (160 μmol m<sup>-2</sup> s<sup>-1</sup>). Dark respiration (*R*) was measured in the last two hours of the night. Six determinations were made per genotype.

**Enzyme assays.** Nitrate reductase (NR) was assayed using around 20 mg of powdered frozen material. Extraction and assay was essentially as in Gibon *et al.* (2004b), including 0 or 10 mM MgCl<sub>2</sub> to distinguish maximal activity (*V*<sub>max</sub>) and the dephosphorylated active form (*V*<sub>sel</sub>).

**qRT-PCR.** RNA was extracted using RNeasy Plant Mini Kit (QIAGEN), genomic DNA removed using TURBO DNA-free Kit (Invitrogen) and cDNA prepared using SuperScript III First-Strand Synthesis System (Invitrogen), in all cases following manufacturer's instructions. Transcripts were quantified by qRT-PCR, including external standards to allow calculation of copy number (Flis *et al.* 2015, 2016).

**Statistics.** *P*-values were calculated in Excel using Student's *t*-test. Analysis of variance between groups (ANOVA) was tested using *aov()* function in R (R Core Team 2017).

Starch degradation rates were calculated by fitting linear regressions between ZT12-24, ZT12-22, ZT12-20 and ZT12-18 to ensure estimates were robust against any slowing of degradation at the end of the night.

Principal component (PC) analysis and canonical correlation (CC) analyses used Z-scored transcript and metabolic data collected at two hour intervals in DAS21 Col-0, *Ws*-2, *gi*, *toc1*, *prp7 prp9* and *lhy cca1* during the LD (light-dark) and second LL of the LLLL (continuous light) treatment. Z-scores were calculated in Excel by calculating the means and standards

deviation of a trait for all samples, subtracting the mean from each sample value and dividing by the standard deviation. Two types analyses were conducted i) treating each genotype as variable and time-series in each trait as observations (Fig. 2, Supplemental Fig. S2A-B, Supplemental Figure S11A) and ii) treating each trait as a variable and time-series in different genotypes as observations (Fig. 7A-D). PC analysis was performed using the `prcomp()` function in R (R Core Team 2017), rescaled coefficients were obtained using `loadings()`, PC scores of each sample were obtained using `scores()` and biplots were generated using `biplot()`.

Canonical correlation (CC) analysis (Hotelling 1936) assesses the relationship between two data sets of multiple variables. It searches for a multivariate axis through one dataset (Canonical Variate X; here, metabolite data) and a multivariate axis through a second dataset (Canonical Variate Y; here, transcript data) such that the two axes are maximally correlated. The pair of axes is termed a canonical function. Following detection of the first canonical function, further correlated pairs of axes are searched for, subject to them being uncorrelated with previous pairs of axes. CC analysis was performed using the `yacca()` function in `yacca` package in R (R Core Team 2017). Canonical redundancy, which describes the proportion of total variance in one dataset that is explained by the other dataset, was obtained using `xvdr()` and `yvdr()` functions. Results were plotted using `helio.plot()` in R (R Core Team 2017) where data bars represent loadings of variables on a given canonical axis. Each canonical axis is a linear combination of the variables in the dataset and the loadings are the relative contributions (i.e. weights) of each variable to the axis.

## Results

### Experimental design

Fig. 1A summarizes the experimental design. Col-0, *Ws-2*, *lhy cca1*, *prp7 prp9*, *toc1* and *gi* were grown for 21 days in a 12 h photoperiod and harvested at 2 h intervals during a light-dark (LD) cycle, after transfer to continuous light for 48 h (LLLL) or after transfer to darkness for 24 h (DD), or after transfer to continuous light for 48 h (LLLL). Experiments with *elf3* used younger plants, because this mutant is early flowering (Zagotta *et al.* 1992). *elf3* and *Ws-2* were grown in a 12 h photoperiod for 12 days and then harvested at 2 h intervals in a LD cycle and after extending the night for 12 h, or after extending the light period for 12 h (LL). Sampling was not continued for longer because *elf3* becomes arrhythmic (Hicks *et al.* 1996; Covington *et al.* 2001). *prp7 prp9*, *toc1* and *gi* are in the Col-0

background and *lhy cca1* and *elf3* are in the Ws-2 background. We measured starch, sucrose, glucose, fructose, glucose 6-phosphate (Glc6P), malate and fumarate (the major organic acids in Arabidopsis; Chia *et al.* 2000; Arrivault *et al.* 2009), total amino acids, protein, chlorophyll a (Chla) and chlorophyll b (Chlb). The data are provided in Supplemental Data files S1-S2.

### **Biomass, rosette composition, photosynthesis and respiration**

All mutants except *gi* accumulated significantly less biomass (both fresh weight, FW and dry weight, DW) than wild-type plants (Fig. 1; Supplemental Fig. S1). FW differences were relatively small for *lhy cca1*, *toc1* and *elf3* (18%, 15%, and 23% lower than wild-type) but substantial for *prp7 prp9* (50% lower than wild-type; Fig. 1B-C). Rosette composition in *lhy cca1*, *prp7 prp9* and *elf3* differed significantly from wild-type plants (2-way ANOVA, genotype effect). Protein and Chl were slightly lower in *lhy cca1*, Chla was slightly lower in *elf3*, and protein and Chla were slightly higher in *prp7 prp9* (Supplemental Figs S1B-D, G-I). Whole rosette photosynthesis on a FW basis (Supplemental Figs S1E, J) resembled wild-type plants in *lhy cca1*, *gi*, *toc1* and *elf3*, and was significantly higher in *prp7 prp9* (Student's t-test,  $p$ -value  $\approx 0.0003$ ) in line with its higher protein and Chl content. The latter needs to be noted in interpreting metabolite data. Respiration (Supplemental Figs S1E, J) was lower in *lhy cca1* (Student's t-test,  $p$ -value  $\approx 0.0005$ ).

### **Global overview of metabolic phenotypes**

We performed principal components (PC) analysis on the dataset described above after Z-score normalization. This was first done for the light-dark cycle (Supplemental Fig. S2A). The analysis separated 13 day-old Ws-2 and *elf3* samples from the 21 day-old plants. We therefore repeated the PC analysis after excluding 13 day-old plants (Fig. 2). PC1 explained 72% and PC2 explained 11% of the variance. *lhy cca1* and *prp7 prp9* were separated in opposite directions along PC1, and Col-0, Ws-2, *gi* and *toc1* grouped together. We also performed PCA on the second 24 h after transfer to continuous light (Supplemental Fig. S2B). PC1 and PC2 explained 42% and 19% of the variance, respectively. There were strong and opposite differences in *lhy cca1* and *prp7 prp9* compared to wild-type plants along PC1, and differences between Col-0, *toc1* and *gi* in PC2. Summarizing, the PC analyses revealed opposed metabolic phenotypes in *lhy cca1* and *prp7 prp9* in both the light-dark cycle and continuous light, whereas the metabolic phenotypes in *gi*, *toc1* and *elf3* were more subtle.

## Diel changes of starch

We inspected the diel changes in individual metabolites in wild-type plants and clock mutants, starting with starch (Fig. 3A-B; Supplemental Figs S3A, S4A). Starch accumulation was significantly slower in *prp7 prp9* and *elf3* than in the corresponding wild-types (Supplemental Table S1;  $p$ -values  $> 0.001$ ). The result for *prp7 prp9* contrasts with previous studies, where starch accumulation in *prp7 prp9* resembled that in wild-type Col-0 (Chew *et al.* 2017). After transfer to continuous light, starch accumulation slowed or plateaued in all genotypes (Supplemental Fig. S3A, see also Fernandez *et al.* 2017).

The rate of starch mobilization was estimated by linear regression between ZT12 and ZT24 for Col-0, Ws-2, *gi*, *toc1*, *prp7 prp9* and *elf3*, and between ZT12 and ZT22 for *lhy cca1*. Degradation was significantly slower in *prp7 prp9* and *elf3* than in the corresponding wild-types (Supplemental Table S1;  $p$ -values  $> 0.001$ ). As previously seen (Graf *et al.* 2010), the short period *lhy cca1* mutant exhausted its starch prematurely before dawn. The other mutants retained significantly more starch than wild-type plants at dawn (starch excess phenotype) (Fig. 3C). The starch excess phenotype was strongest in *prp7 prp9*, moderate in *gi* and *elf3* and slight in *toc1*. Fig. 3D quantifies the altered timing of degradation in the mutants compared to the corresponding wild-type. The regression that was used to estimate the rate of mobilization (see above) was extrapolated to the x-axis to estimate when starch would be depleted. The difference between the extrapolated time of starch depletion in a mutant and the corresponding wild-type is termed St0, with a negative value denoting premature exhaustion and a positive value denoting incomplete exhaustion. St0 was -1.7 h in *lhy cca1* and +0.5, +2.8, +3.0 and +5.1 h in *toc1*, *gi*, *elf3* and *prp7 prp9*, respectively.

## Diel changes of sugars, organic acids and amino acids

Time-series for selected metabolites are shown for 21 day-old Col-0, Ws-2, *prp7 prp9* and *lhy cca1* in Fig. 4, for 13 day-old *elf3* and Ws-2 in Fig. 5, and for all metabolites and mutants in Supplemental Figs S3-S4.

Wild-type plants showed similar diel trends in four separate time-series (21 day-old Col-0, 21 day-old Ws-2, two experiments with 13 day-old Ws-2). Sucrose (Figs 4A, 5A, Supplemental Figs S3B, S4B) increased in the light period, decreased slightly in the night and decreased markedly in the extended night after starch was exhausted (see also Usadel *et al.* 2008; Pal *et al.* 2013). Sucrose was high throughout the subjective day and night in continuous light. Glucose (Fig. 5B, Supplemental Figs S3C, S4C) and fructose (Fig. 5C, Supplemental Figs

S3D, S4D) increased early in the light period, decreased later in the light period and at night, and remained low in the extended night. Glc6P (Figs 4B, 5D, Supplemental Figs S3E, S4E) decreased after dawn, started to rise before dusk and peaked at about ZT14-16. In continuous light, glucose, fructose and Glc6P oscillated with a minimum in the subjective day and a peak in the subjective night that coincided with the time when starch accumulation slowed down (see Supplemental Figs S3A, S4A). Malate (Fig. 4C, Supplemental Figs S3F, S4F) and fumarate (Supplemental Figs S3G, S4G) rose in the light period, decreased to a low value during the night, and remained high in continuous light. Total amino acids (Fig. 4D, Supplemental Figs S3H, S4H) rose in the light period and declined in the night. In continuous light, amino acids remained at a similar level to that at the end of the light period. In contrast to other metabolites, amino acids rose in the extended night.

Many metabolites exhibited changed diel patterns in mutant compared to wild-type plants. ANOVA on entire time-series are provided in Supplemental Table S2. Some of the differences from the wild-type were seen only at specific times in the 24 h cycle. The average change of sucrose and Glc6P between ZT20-24 is summarised Fig. 6A, of sucrose, glucose, fructose and Glc6P between ZT2-ZT10 in Fig. 6B, and of malate, fumarate and nitrate between ZT6- ZT12, and amino acids between ZT14-ZT18 in Fig. 6C.

Metabolite levels in *lhy cca1* were strikingly different from those of wild-type Ws-2, with significant differences for glucose, Glc6P, malate, fumarate, amino acids and nitrate in a light-dark cycle, and for Glc6P, malate and nitrate in the second 24-h cycle in continuous light (ANOVA analysis of the entire time-series,  $p$ -value < 0.05; Supplemental Table S2). There were two major differences. One was at the end of the night when sucrose (Fig. 4A) and Glc6P (Fig. 4B) were transiently and significantly lower in *lhy cca1* than in wild-type Ws-2 (Fig. 6A). This transient response coincided with the premature depletion of starch (see above) and was smaller in continuous light, consistent with it being a consequence of the changed pattern of starch turnover. The second major difference was that *lhy cca1* contained significantly lower levels of malate, fumarate and total amino acids than Ws-2 (Supplemental Fig. S3F-I); malate and fumarate were significantly lower for most of the light-dark cycle (Figs 4C-D; Supplemental Table S3), and amino acids were significantly lower between ZT4-ZT12 (Supplemental Fig. S3F-H, Fig. 6C). Nitrate was significantly higher in *lhy cca1* than wild-type Ws-2 (Supplemental Fig. S3I, Supplemental Table S2). These differences were retained as trends in continuous light, although mainly non-significant (Fig. 4, Supplemental Fig. S3).

Metabolite levels in *prp7 prp9* were different from those of wild-type Col-0, with significant changes of sucrose, Glc6P, malate, fumarate, nitrate and amino acids in both the light-dark cycle and in continuous light (ANOVA of the entire time-series,  $p$ -value < 0.05; Supplemental Table S2). The differences between *prp7 prp9* and Col-0 were broadly reciprocal to those between *lhy cca1* and Ws-2. Compared to Col-0, *prp7 prp9* showed transiently elevated sucrose (Fig. 4A, see Supplemental Fig. S5B for a replicate experiment), glucose (Supplemental Figs S3C, S5C) and Glc6P (Fig. 4B) during the first part of the light period, and elevated sucrose and Glc6P during the night (Fig. 4A-B). Sucrose was also elevated in *prp7 prp9* relative to wild-type Col-0 in continuous light (Fig. 4A). Malate and fumarate (Fig. 4C, Supplemental Fig. S3G, Fig. 6C) were elevated in *prp7 prp9* throughout the light-dark cycle, in the first hours of the extended night, and in continuous light. Amino acids (Fig. 4D) were significantly elevated in the last part of the light dark cycle and early in the night in a light dark cycle (see also Fig. 6C) and in continuous light, especially between ZT24-34 (Fig. 4D).

The metabolic phenotype in *toc1* and *gi* was much weaker than that of *lhy cca1* or *prp7 prp9*. The weak changes were mostly in the same direction as those in *prp7 prp9* (Fig. 6; Supplemental Figs. S3B-H); Supplemental Table S2). Compared to wild-type Col-0, *toc1* showed significantly increased Glc6P in light-dark cycles and increased fumarate in continuous light, and *gi* showed significantly increased fumarate in light-dark cycles and increased sucrose, Glc6P, malate and fumarate in continuous light.

The metabolic phenotype of *elf3* contrasted with that of the other mutants. In the light period, *elf3* contained similar sucrose (Fig. 5A, Supplemental Fig. S4B, Supplemental Table S2, Fig. 6B) and substantially and significantly higher glucose, fructose and Glc6P (Fig. 5B-D, Fig. 6, Supplemental Fig. S4C-E; Supplemental Table S2) than wild-type Ws-2. These metabolites decreased to levels like those in wild-type Ws-2 in the night, and also in the extended light treatment. A separate experiment confirmed that glucose, fructose and Glc6P were higher in the first part of the T-cycle in *elf3* than in wild-type plants (Supplemental Fig. S4C-E). Malate, fumarate, amino acid and nitrate in *elf3* resembled wild-type Ws-2 (Supplemental Fig. S4F-I, Fig. 6B).

The oscillation in Glc6P seen in wild-type plants in continuous light was present in the circadian clock mutants (Figs 4B, 5D, Supplemental Fig. S3E). Compared to wild-type



plants, this oscillation appeared to have a shorter period in *lhy cca1* and a longer period in *prp7 prp9*.

### **Diel changes of further metabolites**

We profiled more phosphorylated intermediates and organic acids in *lhy cca1*, *toc1*, *gi*, *prp7 prp9*, *elf3* and the corresponding wild-types at the end of the night (EN) and the end of the light period (ED) (Supplemental Fig. S6, Supplemental Data file S3) and in *elf3* throughout the light-dark cycle (Supplemental Fig. S8, Supplemental Data file S3). We also analyzed individual amino acids throughout the light-dark cycle in Col-0, Ws-2, *lhy cca1*, *toc1*, *gi* and *prp7 prp9* (Table 1, Supplemental Fig. S7, Supplemental Data file S4).

The premature exhaustion of starch and transient decrease in sucrose and Glc6P at the end of the night in *lhy cca1* was accompanied by further changes that are typical of C starvation (see Usadel *et al.* 2008). At the end of the night *lhy cca1* had 10-fold lower levels of the sucrose-signal trehalose 6-phosphate (Tre6P) and lower levels of many glycolytic intermediates (UDPglucose, Glc1P, 3-PGA, phosphoenolpyruvate, pyruvate) and organic acids (citrate, aconitate, isocitrate, 2-oxoglutarate) than wild-type Ws-2 (Table 1; Supplemental Fig. S6, all significant at  $p < 0.05$ ), and significantly higher levels of Asn and many minor amino acids (Leu, Ileu, Val, Arg, Trp, Tyr, Phe, Lys) (Table 1, Supplemental Fig. S7H, I-J, L-Q; Supplementary Data File S4).

The low level of malate and fumarate at the end of the day in *lhy cca1* compared to Ws-2 (see above) was accompanied by a trend to lower levels of other organic acids (Table 1, Supplemental Fig. S6O-R, significant at  $p < 0.05$  for 2-oxoglutarate and glycerate). The low total amino acid content in *lhy cca1* at the end of the day (see above, Figs 4D, 6C) was mainly due to significantly lower levels of major amino acids like Gln, Gly and Ser compared to wild-type Ws-2 (Supplemental Fig. S7A–B, S7E–F, Supplementary Data File S4, Student's t-test and ANOVA,  $p < 0.05$ ;  $p < 0.05$  for Ser at multiple time points, not shown). Some minor amino acids including Cys and cystathione were also significantly lower compared to wild type (Supplemental Fig. S7A, S7E–F, significant in ANOVA at  $p < 0.05$ ). Nitrate rose towards dusk (Supplemental Fig. S3I) indicating a restriction on nitrate assimilation.

The high malate and fumarate levels at the end of the day in *prp7 prp9* were accompanied by high levels of other organic acids like citrate, isocitrate and aconitate, compared to wild-type Col-0 (Table 1, Supplemental Fig. S6O–Q, all significant at  $p < 0.05$ ). The high total amino

acid content during the night in *prp7 prp9* (see above, Fig. 4D) was mainly due to high levels of central amino acids like Glu, Asp and Ser, compared to Col-0 (Supplemental Fig. S7B, D, F,  $p < 0.05$ ). Many minor amino acids including Thr, Lys, His, Val, Leu, Ileu, Cys and Hser were significantly elevated in *prp7 prp9*, at the end of the light period and in the first part of the night (Supplemental Fig. S7, Supplementary Data File S4,  $p < 0.05$  in ANOVA and Student's t-test). However, whereas aromatic amino acids (Phe, Tyr, Trp) peaked at dusk in other genotypes, they remained low in *prp7 prp9* (Table 1, Supplemental Fig. S7O-Q,  $p < 0.01$ ).

The high Glc6P in the first part of the light period in *elf3* compared to Ws-2 was accompanied by higher levels of other sugar phosphates including Glc1P and UDPGlc (Supplemental Fig. S8C-G, significant at  $p < 0.01$ ) and the sucrose-signal Tre6P (Table 1, Supplemental Fig. S6A, S8A, significant at  $p < 0.001$ ). Organic acids did not differ between *elf3* and Ws-2 (Table 1, Supplemental Fig. S8H-Q). *toc1* and *gi* were not markedly different from wild-type plants (Supplemental Figs S6, S7).

Summarizing, Figs 2-6 and Supplemental Figs S2-S8 reveal several impacts of altered circadian clock function on central metabolism. These include: (i) altered timing of starch degradation in all five circadian clock mutants, especially *lhy cca1* where starch is prematurely exhausted and *prp7 prp9* and *elf3* where there is a large starch excess at dawn. (ii) A transient decrease of sugars, Glc6P, many other phosphorylated metabolites and organic acids and a rise in minor amino acids around dawn in *lhy cca1*, which coincides with premature exhaustion of starch and is indicative of transient C-starvation. The low respiration rate in *lhy cca1* might also be linked to C starvation. (iii) Slower starch accumulation in *prp7 prp9* and *elf3* even though these mutants have similar or higher levels of sucrose and/or reducing sugars than wild-type plants in the light. (iv) Higher organic acids and amino acids in the later part of the light period and at night in *prp7 prp9* and lower levels of these metabolites in *lhy cca1*. (v) Elevated levels of reducing sugars and Glc6P in the first part of the T-cycle in *elf3*.

### **Multivariate analysis of the responses of metabolites and circadian clock transcripts**

Data for transcript abundance of ten circadian clock genes in the same plant material were published previously (Flis *et al.* 2015, data replotted in Supplemental Figs S9-S10). We performed two multivariate analyses to identify relationships between metabolite levels and circadian clock transcript abundance: PC analysis and canonical correlation (CC) analysis

(Figs 7, 8). We used data collected at 2 h intervals in 21 day-old Col-0, Ws-2, *gi*, *toc1*, *prp7*, *prp9* and *lhy cca1* during the light-dark cycle and the second 24 h of the continuous light treatment. We excluded 13-day-old Ws-2 and *elf3* for two reasons. First, their inclusion would introduce plant-age effects; the 13-day-old plants grouped separately to 21-day-old plants in a PC analysis performed on metabolite data (Supplemental Fig. S2, see also Supplemental Fig. S11A for an analogous PC analysis on the combined metabolite and transcript data). Second, excluding *elf3* allowed us to compare time-series in light-dark cycles and continuous light.

PC analysis was performed to search for interactions between the individual traits, i.e. the 10 transcripts and 12 metabolites. The vector biplots in Fig. 7 display the loadings of each variable in PC1 and PC2. Variables with vectors pointing in the same direction are positively correlated, variables with vectors pointing in opposite directions are negatively correlated, and variables with vectors at 90 degrees to each other are uncorrelated between genotypes.

In the analysis of the light-dark dataset, PC1 and PC2 represented 37% and 22% of the variance, respectively (Fig. 7A). PC1 and PC2 were driven mainly by circadian clock progression through the 24 h cycle and diel turnover of metabolites; the vectors for circadian clock transcripts showed a clockwise distribution that resembled the time at which they peak during a light dark cycle, and the vectors for starch, sucrose, malate, fumarate and total amino acids were closely aligned. We therefore inspected PC3 and PC4 to find variance that might be independent of diel changes (Fig. 7B). PC3 and PC4 accounted for 12% and 6% of variance, respectively. *LHY* and *CCA1* transcripts correlated positively with fumarate, malate, glucose and fructose, consistent with the dawn components positively regulating organic acid metabolism. *ELF4* transcript correlated negatively with *LHY*, *CCA1*, *PRR9* transcripts and malate, fumarate, glucose and fructose, indicating *ELF4* may counteract the positive action of dawn components on these metabolites. *TOC1* transcript correlated positively with total protein and nitrate, and negatively with malate, fumarate, glucose, fructose and total amino acids. However, this effect is likely to be secondary because these metabolites did not show large changes in the *toc1* mutant (see above). *PRR7* and, more weakly, *GI* and *PRR5* transcripts correlated negatively with starch and sucrose.

We also performed PC analysis on the second 24 h of the continuous light treatment, with the aim of focusing on circadian regulation by removing diel changes. This analysis was compromised because most metabolites showed smaller amplitudes than in a light-dark cycle.

PC1 and PC2 accounted for 25% and 20% of total variance, respectively. The biplot (Fig. 7C) had a counter-clockwise distribution of the circadian clock transcript vectors reflecting clock progression through the cycle. The vectors of circadian clock transcripts were mostly unrelated to those of metabolites. *PRR7* transcript exhibited a negative correlation with glucose and a weaker negative correlation with fructose, Glc6P and Chlb. PC3 and PC4 accounted for 9 and 8% of total variance, respectively (Fig. 7D). *LHY* and *CCA1* transcripts correlated positively with protein, more weakly with malate, fumarate and amino acids, and negatively with starch, *ELF3* transcript correlated positively with starch. *PRR9*, *PRR7* and *PRR5* transcripts correlated positively with amino acids and negatively with starch, Glc6P and nitrate.

CC analysis (Hotelling 1936) was performed to detect global relationships between transcript profiles and metabolic traits. Whereas PC analysis searches for relationships between all of the individual traits in a multivariate data set, CC analysis assesses the relationship between two datasets of multiple variables. The proportion of total variance in one dataset that is explained by the other dataset is quantified as the redundancy index, which is calculated for each canonical variate in each canonical function (Stewart & Love 1968).

CC analysis of the light-dark cycle dataset detected very high correlations between the transcript and metabolite datasets (Fig. 8). The summed redundancy coefficients for all detected canonical functions were 29.6 and 46.9 for X|Y variables and Y|X variables, respectively, indicating that metabolite data explained about 30% of total variance in transcript data and transcript data explained about 47% of total variance in metabolite data. Most variance was captured in the first three canonical functions (summed redundancy index of 22.7 and 38.9 for X|Y variables and Y|X variables, respectively). Correlations in these three pairs of canonical axes were strong and highly significant (0.87, 0.82, 0.70, all  $p$ -value < 0.001). Each is presented as a heliplot, displaying the loadings of each individual variable with the X or Y canonical variate (Fig. 8).

The first canonical function accounted for 9% and 24% of total variance for X|Y variables and Y|X variables respectively. It was driven by the timing of the peaks for transcripts and metabolites in the diel cycle (Fig. 8A). This is shown by the loading gradient for the circadian clock genes (Y variables) which changes from strongly negative for *LHY* and *CCA1* transcripts to weakly negative for *PRR9*, weakly positive for *PRR7* transcript and strongly positive for most dusk and EC transcripts. The low *ELF3* loading might reflect the relatively

weak circadian oscillation of its transcript (Flis *et al.* 2015, see Supplementary Fig. S9). On the metabolite axis, starch, malate and total amino acids had high positive loadings and Chla, Chlb, fumarate and total protein had lower positive loadings.

The second canonical function (Fig. 8B) accounted for 10% and 12% of total variance for X|Y variables and Y|X variables, respectively. It detected a link between circadian clock components and C metabolism. On the transcript axis, *PRR7* and *GI* had the highest positive loadings, *PRR9*, *LUX* and *ELF4* had lower positive loadings, and *ELF3* showed a negative loading. Of the metabolites, Glc6P had a negative loading and glucose and fructose had positive loadings. These results and our PC analyses are in agreement with previous reports of an interaction between carbohydrate metabolism and *GI* and *PRR7* (Dalchau *et al.* 2011; Haydon *et al.* 2013) but additionally indicate that *PRR9*, *LUX*, *ELF4* and *ELF3* might be interlocked in the regulatory loop. *ELF3* appears to act in an opposite direction to the other circadian clock components. It is noteworthy that the link between *ELF3* and reducing sugars that we uncovered in the *elf3* mutant (Figs 3, 5, 6) is recapitulated in this multivariate analysis, even though the data set that does not contain data from the *elf3* mutant.

In the third canonical function (Fig. 8C) *LHY*, *CCA1*, *PRR5* and *GI* had positive loadings on the transcript axis. On the metabolic axis malate, fumarate, Glc6P and Chlb had high positive loadings and nitrate and total protein had negative loadings. This points to a link between *LHY*, *CCA1*, *PRR5* and *GI* and organic acid metabolism.

We also performed CC analysis on the second 24 h interval of the continuous light treatment (Supplemental Fig. S11B), focusing on the first two canonical axes, which explained 10% of the variation in metabolites, and 22% of the variation in transcripts. In the first canonical axis, *CCA1*, *PRR9*, *PRR7*, *PRR5* and *GI* had high positive and *ELF3* negative weightings on the Y-axis. Starch, sucrose, glucose, fructose, Glc6P and fumarate had negative weightings on the X-axis. In the second canonical axis, *LHY*, *CCA1* and *PRR9* had negative weightings and most of the dusk and evening circadian clock components had positive weightings on the Y-axis, whilst starch, malate and amino acids had positive weightings on the X-axis.

These multivariate analyses pointed to many relationships between individual, and more commonly sets of, circadian clock components and metabolic traits. We performed further experiments and data analyses to explore two of them in more detail.

## Comparison of changes in the timing of starch degradation and circadian clock period

For starch, the most marked phenotype was the differing starch content at dawn. This was mainly due to differences in the timing, rather than the rate, of starch degradation (Fig. 3, Table S1). It has been proposed that starch mobilization is paced to dawn, as anticipated by the circadian clock (see Introduction). To test this idea, we analyzed the transcript data set for each mutant to define the shift in circadian clock period relative to the corresponding wild-type. To do this, we measured the distance between the transcript peak in the first and second LLLL cycle for each circadian clock gene (Fig. 9A, Supplemental Fig. S10) and then, for a given mutant, averaged the values for all circadian clock genes to estimate period for that mutant (Supplemental Table S3). Compared to Col-0 and Ws-2 (25.4 and 24.5 h, respectively), period was strongly lengthened in *prp7 prp9* (30.3 h), slightly lengthened in *gi*, (25.7 h), slightly shortened in *toc1* (23.4 h) and strongly shortened in *lhy cca1* (21.7 h). These estimates of period length largely resemble those reported previously (Somers *et al.* 1998; Mizoguchi *et al.* 2002; Salomé & McClung 2005; Martin-Tryon *et al.* 2007). The analysis could not be performed for *elf3* because it is arrhythmic in continuous light (Hicks *et al.* 1996; Covington *et al.* 2001).

We compared these shifts in period length with St0 (the shift in the time at which starch is exhausted in a mutant, compared to the relevant wild-type, Fig. 3D). Regression of St0 against the shift in circadian clock period revealed a strong positive correlation ( $R^2 \approx 0.91$ ) (Fig. 9B). The correlation was driven mainly by *lhy cca1* and *prp7 prp9*. The pattern of starch degradation in *gi* and *toc1* may not be fully explained by circadian clock period. Compared to wild-type Col-0, *gi* had a large delay in St0 (+2.8 h) but only a small increase in circadian clock period (+0.3 h), and *toc1* had a delay in St0 (+ 0.5 h) but a shorter circadian clock period (-2 h) than wild-type plants. However, this deviation may be within the range of experimental error.

## Comparison of changes in the timing of starch degradation and the rise of dawn transcripts in a light-dark cycle

Starch degradation occurs in the dark. We therefore inspected the time courses for circadian clock transcripts in the various mutants in light-dark cycles, with a particular focus on when dawn transcripts peaked (Fig. 9C, Supplemental Fig. S9). In the short period *lhy cca1* mutant, circadian clock transcripts peaked about 4 h earlier than in Ws-2. *LHY* and *CCA1* were not



available as dawn markers in this mutant, but other dawn markers like *GBSSI* are expressed in *lhy cca1* about 4 h before dawn under growth conditions similar to our experiments (Graf *et al.* 2010). In the *toc1* mutant all genes including *LHY* and *CCA1* peaked 1-2 h earlier than in Col-0. In *gi*, most transcripts showed a slight delay compared to Col-0. In *elf3*, the peaks of transcripts for dawn genes were delayed by 1-3 h relative to wild-type. In *prp7 prp9*, transcript peaks were delayed by about 5 h for the dusk and evening genes but, unexpectedly, there was no delay for the dawn genes *LHY* and *CCA1*. These peaked around ZT24, at about the same time as wild-type plants (Fig. 9C).

Fig. 9D compares St0 with the shift in the time when dawn is anticipated by the circadian clock in a light-dark cycle. The latter was defined as the shift in peak transcript abundance for the *LHY* and *CCA1* transcripts, except for *lhy cca1* where an advance of 4 h was estimated based on the observed response of *GBSSI* transcript abundance (Graf *et al.* 2010) and the advance of all other circadian clock gene transcripts in our dataset (see Fig. 9C). The shift in St0 resembled the shift in the circadian clock dawn response in *lhy cca1*, *elf3* and *gi*. A small discrepancy arose for *toc1* where St0 was slightly delayed but the time at which dawn was anticipated was advanced. There was a large discrepancy for *prp7 prp9*, where St0 was strongly delayed but *CCA1* and *LHY* transcripts peaked at the same time as in wild-type Col-0.

We asked why *CCA1* and *LHY* transcript abundance peaked at around ZT24 in *prp7 prp9* in a light-dark cycle (Fig. 9C-D) despite this mutant having a long period in continuous light (Fig. 9A-B; see also Supplemental Table S3). Whereas *LHY* and *CCA1* transcripts decrease rapidly after dawn in wild-type plants, they remained high until the end of the light period in *prp7 prp9* (Fig. 9E, see also Supplemental Fig. S9A-B). This stabilization of *CCA1* and *LHY* transcripts in *prp7 prp9* is due to loss of the repressor function of the day genes (Pokhilko *et al.* 2012; Fogelmark & Troein 2014). Sustained expression of the dawn genes in *prp7 prp9* explains the strong delay in the rise and, in continuous light, the delay in the decay of dusk and EC transcripts (Fig. 9F-G, see also Supplemental Fig. S9F-J). In a light dark cycle, however, darkening leads to a rapid decrease of *PRR5*, *TOC1* and EC transcripts. This will de-repress *LHY* and *CCA1* and may explain why dawn transcripts rise at almost the same time in *prp7 prp9* as in wild-type Col-0. Thus, in *prp7 prp9*, clock progression is delayed in the first part of the light-dark cycle but accelerates after dusk. This contrasts with continuous light, when progression is delayed over the whole 24 h cycle. The unexpected response in

*prp7 prp9* indicates that the starch degradation is paced by a circadian clock output that occurs before the end of the light period.

### **Circadian clock mutants slow down starch degradation after a sudden early dusk**

The above analyses indicated that the pacing of starch mobilization to dawn does not depend solely on the dawn genes or, indeed, any single circadian clock component. To further investigate whether the timing of starch mobilization depends on individual circadian clock components, wild-type Col-0 and Ws-2 and four clock mutants were grown in a 12 h photoperiod and subjected to a sudden early dusk (darkness at 8 or 9 h instead of 12 h after dawn: Supplemental Fig. S12). One set of experiments was performed using 21 day-old plants of Col-0, Ws-2, *lhy cca1*, *prp7 prp9*, and *toc1* and another set with 13 day-old Ws-2 and *elf3*. The mutants showed the same starch phenotype at dawn as in Fig. 3; namely, *lhy cca1* exhausted its starch prematurely whereas starch was not fully exhausted at dawn in *toc1*, *elf3* and especially *prp7 prp9*. After a sudden early dusk, wild-type Col-0 and Ws-2 slowed down mobilization by 33-42% compared to unperturbed plants ( $p < 0.001$ , Table 2) and starch reserves lasted until dawn as previously reported (Graf *et al.* 2010; Scialdone *et al.* 2013; Martins *et al.* 2013). All four circadian clock mutants also slowed down mobilization after a sudden early dusk, although to varying extents (32, 18, 28 and 41% lower in *lhy cca1*, *prp7 prp9*, *toc1* and *elf3*,  $p < 0.001$ , 0.05, 0.05 and 0.001, respectively, Table 2).

### **Comparison of diel responses of organic acids and amino acids with the response of circadian clock transcripts in *lhy cca1* and *prp7 prp9***

As described above, organic acids and amino acids were lower in *lhy cca1* and higher in *prp7 prp9* than in wild-type plants (Fig. 4C-D, Supplementary Fig. S3G) and multivariate analysis indicated links between *LHY* and *CCA1* and malate, fumarate and total amino acid levels (Figs 7A-B, 8A, 8C). Inspection of the transcript abundance time-series revealed that the opposing response of organic acids and amino acids in *lhy cca1* and *prp7 prp9* match changes in *LHY* and *CCA1* expression (Supplemental Figs S9-S10, see also Fig. 9E-G). Expression of *LHY* and *CCA1* was abolished in *lhy cca1*, and was sustained for much longer in *prp7 prp9*. This contrasted with expression of *PRR7* or *PRR9*, which was abolished in *prp7 prp9*, and decreased in *lhy cca1* compared to wild-type Ws-2 (Supplemental Figs S9-10, see also Supplemental Fig. S13 for independent confirmation).

### Organic acids and amino acids in *lhy cca1* in a T-17 cycle

C starvation represses and post-translationally inactivates NR and inhibits amino acid synthesis (Vincentz *et al.* 1993; Campbell 1999; Stitt *et al.* 2002; Figueroa *et al.* 2016). We asked whether the low levels of organic acid and amino acids between ZT6 and ZT14 in *lhy cca1* might be a consequence of premature exhaustion of starch and C-starvation around dawn. One argument against this idea is that malate, fumarate and amino acids were low in *lhy cca1* and high in *prp7 prp9* in continuous light (see above). As an independent test, we grew wild-type Ws-2 and *lhy cca1* in a T-17 cycle (8.5 h light, 8.5 h dark) (Fig. 10, Supplemental Fig. S14), where the external light dark cycle is close to the period of *lhy cca1*. At dawn in a T-17 cycle, *lhy cca1* contained more starch (7.6  $\mu\text{mol}$  glucose equivalents/g FW) than wild-type Ws-2 at dawn in a 24 h T-cycle (3-5  $\mu\text{mol}$  glucose equivalents/g FW Supplemental Fig. S14B) and similar levels of sucrose, glucose and Glc6P to those in wild-type Ws-2 in a T-24 or a T-17 cycle (Supplemental Fig. S14C-E). Sucrose, glucose and Glc6P were slightly lower in *lhy cca1* than Ws-2 at some early times in the light but there was no significant difference from ZT6 onwards (Supplemental Fig. S14J-L). Crucially, *lhy cca1* in a T-17 cycle had lower levels of malate and fumarate than Ws-2 throughout the light period (Fig. 10A-B), and amino acids were lower from ZT8 onwards (Fig. 10C, see also Supplemental Fig. S14F-H). We conclude that mistiming of starch degradation is not the main reason for the differing levels of organic acids and amino acids between *lhy cca1* and wild-type plants and, by inference, *prp7 prp9*.

### Nitrate reductase activity in *lhy cca1* and *prp7 prp9*

The higher level of nitrate and lower levels of amino acids at ZT8-12 in *lhy cca1* relative to wild-type plants and the opposing response in *prp7 prp9* point to modification of nitrate assimilation. We investigated NR activity at dusk (Fig. 11) using two assays; in the absence of  $\text{Mg}^{2+}$  ( $=V_{\text{max}}$ ) and in the presence of  $\text{Mg}^{2+}$  to allow binding of an inhibitory 14-3-3 protein to phosphorylated nitrate reductase ( $=V_{\text{sel}}$ ) (Kaiser & Huber 2001; Lillo *et al.* 2004).  $V_{\text{sel}}$  in *lhy cca1* resembled that in Ws-2, but  $V_{\text{sel}}$  in *prp7 prp9* was two-fold higher than in wild-type Col-0 (Fig. 11A). The ratio of  $V_{\text{sel}}/V_{\text{max}}$ , which is a measure of post-translational activation, was higher in *prp7 prp9* and marginally lower in *lhy cca1* than in wild-type plants (Fig. 11B).

## Discussion

### Central metabolism is regulated by several circadian clock outputs

We have carried out time-resolved analyses of starch and major intermediates in central metabolism in light-dark cycles and continuous light in five circadian clock mutants (*lhy cca1*, *prp7 prp9*, *toc1*, *gi*, *elf3*), chosen to investigate the impact of lesions in dawn, day, dusk and evening clock components. Our analyses uncover many changes in central metabolism (Fig. 12) including; (i) slower starch accumulation in *prp7 prp9* and *elf3*, (ii) higher reducing sugars early in the T-cycle in *elf3*, (iii) a modified pattern of starch mobilization with *lhy cca1* exhausting starch prematurely whilst *toc1*, *gi*, *elf3* and especially *prp7 prp9* show a starch excess phenotype at dawn and (iv) lower organic acids and amino acids in the middle of the T-cycle in *lhy cca1* and higher levels of these metabolites in *prp7 prp9*.

The metabolic phenotypes were often weak compared to the strong developmental phenotypes exhibited by many of these mutants. The metabolic phenotypes were also less pronounced than those seen when clock-associated genes like *TIC* (Sanchez-Villareal *et al.*, 2013) are mutated. These comparisons point to compensatory or buffering capacity within the circadian clock. As the circadian clock operates in a highly integrated manner, phenotypic changes in a given mutant may anyway not be a direct consequence of the deleted component. We therefore integrated our metabolite data with data for the responses of ten circadian clock transcripts in the same plant material (Flis *et al.* 2015) to explore which clock components underlie these metabolic phenotypes.

### Starch accumulation is slower in *elf3* and in *prp7 prp9*

Plants accumulate starch more quickly in short than in long photoperiods to provide a larger C reserve to support maintenance and growth in the long night (Smith & Stitt 2007; Sulpice *et al.* 2014b; Mengin *et al.* 2017). It has been proposed that the higher rate of starch accumulation is due to a restriction of growth in the light period in response to short photoperiods or low C availability in the preceding night (Sulpice *et al.* 2014b; Mugford *et al.* 2014; Mengin *et al.* 2017). There was previously no evidence that the circadian clock regulates the rate of starch accumulation (Mugford *et al.* 2014).

Our data reveal that the clock contributes to the regulation of starch accumulation. In particular, accumulation is significantly slower in *elf3* and *prp7 prp9* than in wild-type plants

(Fig. 3; Supplemental Table S1). This is not due to a lower rate of C fixation; photosynthesis was as high in *elf3* and higher in *prp7 prp9* than in wild-type plants (Supplemental Fig. 1E,J). It is also not a secondary effect due to excessive use of C for growth; sucrose and reducing sugars in *prp7 prp9* and *elf3* in the light were as high or even higher than in wild-type plants (see below for more discussion).

One possible explanation for the slow starch accumulation in *prp7 prp9* and *elf3* would be that these mutants do not exhaust their starch during the night, and that this results in slower starch accumulation in the light period. However, the slower rate of starch accumulation in wild-type plants when they are grown in long photoperiods or under high irradiance is accompanied by lower levels of reducing sugars (Mengin *et al.* 2017; see below for more references), which is opposite to the metabolic phenotype in *prp7 prp9* and, especially, *elf3*. This indicates that the day genes or *ELF3* have a more direct action on starch accumulation.

Integration of the starch time-series and the circadian clock transcript time-series indicates that *ELF3* is a positive regulator of starch accumulation, and that the slow starch accumulation in *prp7 prp9* is a secondary effect due to delayed expression of *ELF3* or other EC components in *prp7 prp9*. The rise of *ELF3*, *ELF4* and *LUX* transcripts is strongly delayed in *prp7 prp9* compared to wild-type plants (Supplemental Fig. S9H-J). This can be explained by the sustained repressor function of LHY and CCA1 in this mutant. On the other hand, in the *elf3* mutant the decrease of *PRR7* transcript in the night is almost completely abolished and *PRR9* transcript increases earlier than in wild-type plants (Supplemental Fig. S9M-N). This is expected from the EC's repression of *PRR9* and other circadian clock genes (Nusinow *et al.* 2011; Dixon *et al.* 2011; Helfer *et al.* 2011; Herrero *et al.* 2012; Mizuno *et al.* 2014). Thus, the slow starch accumulation in *elf3* and *prp7 prp9* is consistently associated with decreased or abolished *ELF3* expression, whereas there is no consistent relation with *PRR7* or *PRR9* expression. The idea that slow starch accumulation in *prp7 prp9* is a secondary effect would also explain why starch accumulation is not always slowed down in *prp7 prp9* (Chew *et al.* 2017).

Seaton *et al.* (2014) proposed three variants in their model for the circadian regulation of starch turnover. Two variants assumed for simplicity that there would be little change in the rate of starch accumulation in circadian clock mutants compared to wild-type plants. The third allowed action of the circadian clock on accumulation as well as degradation, and predicted slower starch accumulation in *elf3* than in wild-type plants.

*ELF3* interacts with *ELF4* and *LUX* to form the EC (Nusinow *et al.* 2011; Dixon *et al.* 2011; Helfer *et al.* 2011; Herrero *et al.* 2012; Mizuno *et al.* 2014). Although *ELF3* has a fairly broad expression peak, EC is thought to be active in the middle of the 24 h cycle, when transcripts peak for the other EC components (*ELF4*, *LUX*) (Nusinow *et al.* 2011; Flis *et al.* 2015, see Supplemental Figs S9-10). Starch accumulation in *elf3* was already slower early in the light period (Fig. 3B, Supplemental Fig. S4A). This implies that there is a marked delay between primary activity of EC and the restriction of starch accumulation, or that *ELF3* is acting via an EC-independent pathway like that identified in Nieto *et al.* (2015).

### ***ELF3* negatively regulates levels of reducing sugars early in the 24 h cycle**

The *elf3* mutant had similar or marginally increased levels of sucrose, strongly elevated glucose and fructose, and elevated levels of many phosphorylated intermediates between ZT2-10 relative to wild-type plants (Fig 5, Supplemental Figs S4, S8). The increase of reducing sugars in *elf3* differed from the metabolic phenotypes in *lhy cca1* and *prp7 prp9*; the increase was much larger, it was mainly for glucose and fructose, it was restricted to the first part of the 24 h cycle and disappeared after ZT8, and it occurred independently of changes in organic acids or amino acids. Multivariate analysis also pointed to *ELF3* having a distinctive impact on reducing sugars (Fig. 8). As already discussed for starch accumulation, there may be a delay between the activity of EC and the inhibition of sucrose hydrolysis, or *ELF3* may act via an EC-independent pathway to prevent hydrolysis of sucrose to reducing sugars.

A transient increase of reducing sugars in the first part of the light period occurs in many species including tobacco (Scheible *et al.* 2000), potato (Urbanczyk-Wochniak *et al.* 2005) and Arabidopsis (Gibon *et al.* 2006; Sulpice *et al.* 2014b). In Arabidopsis this increase becomes more marked in short photoperiods (Sulpice *et al.* 2014b; Mengin *et al.* 2017) or after extending the night (Gibon *et al.* 2004b). It may contribute to the increased allocation of photosynthate to starch in these conditions. Increased hydrolysis of sucrose to reducing sugars and their phosphorylation to hexose phosphates decreases the net rate of sucrose synthesis, and the rise in hexose phosphate will trigger feedback regulation of the cytosolic fructose biphosphate and promote starch synthesis (Huber & Huber 1996; Trevanion *et al.* 2004; Stitt *et al.* 2010).

In *elf3*, however, starch accumulation was slower than in wild-type plants even though there were elevated levels of reducing sugars and sugar phosphates. Our results therefore indicate that *ELF3* exerts a dual influence on starch accumulation; a stimulatory effect on starch



accumulation (see last section) and an indirect antagonistic effect by suppressing the rise of reducing sugars. These outputs may be in part independent and separately modulated.

Hydrolysis of sucrose to reducing sugars may have further functions in addition to increasing starch accumulation. The transient peak of reducing sugars at about ZT4 coincides with a maximum in the circadian oscillation in rosette expansion (Poiré *et al.* 2010; Dornbusch *et al.* 2014; Apelt *et al.* 2015, 2017). EC plays an important role in the circadian regulation of extension growth in hypocotyls (Nozue *et al.* 2007) and roots (Yazdanbakhsh *et al.* 2011). By repressing *PIF4* and *PIF5*, EC inhibits extension growth in the middle of the T-cycle, and this inhibition is relieved before dawn when EC activity decreases and *PIF4* and *PIF5* expression rise (Nusinow *et al.* 2011). Furthermore, *PIF4* and *PIF5* regulate genes involved in auxin synthesis and cell expansion, and several invertases and putative invertase inhibitors (Hornitschek *et al.*, 2012). These observations prompt the hypothesis that sucrose hydrolysis might be involved in providing energy and increasing turgor during expansion growth and that *ELF3* negatively regulates this process.

### **An integrated circadian clock output paces starch mobilization to anticipated dawn**

The clock has a pervasive influence on starch degradation (Fig. 3, Supplemental Figs S3, S4). Our results confirm earlier reports that starch is prematurely exhausted in the short period mutant *lhy cca1* (Graf *et al.* 2010; Scialdone *et al.* 2013) and incompletely mobilized at dawn in *prp7 prp9* (Chew *et al.* 2017) and *gi* (Rédei 1962; Eimert *et al.* 1995; Messerli *et al.* 2007) and show that starch is incompletely mobilized in *toc1* and *elf3*.

Graf *et al.* (2010) proposed that the circadian clock sets the rate of degradation such that starch is almost but not completely exhausted at dawn. This allows the plant to maximize growth in a fluctuating environment whilst avoiding premature exhaustion of starch and deleterious periods of C starvation at the end of the night (Graf & Smith 2011; Stitt & Zeeman 2012; Greenham & McClung 2015). Current models (Graf & Smith 2011; Scialdone *et al.* 2013; Seaton *et al.* 2014) propose that a circadian clock output sets a 'Timer', providing information about the time to dawn, named T. This is integrated with information about the amount of starch, S, in an arithmetic division to set the rate of starch degradation. We used our time-resolved data to estimate when the initial rate of starch degradation would exhaust starch in the various circadian clock mutants, compared to wild-type plants (St0, Fig. 3D). In agreement with the models of Scialdone *et al.* (2013) and Seaton *et al.* (2014), there was a

good match between St0 and the shift in circadian clock period, estimated from the time when clock transcripts peaked in continuous light (Fig. 9A-B). Generally, both were advanced in *lhy cca1*, and both were delayed in mutants with lesions in the day, dusk and evening clock components. Furthermore, circadian clock mutants were able to decrease the rate of starch degradation after a sudden early night (Supplemental Fig. S12). Together, these results confirm that starch mobilization is paced to dawn as anticipated by the circadian clock, and show that the circadian clock is still able to rapidly adjust the rate of degradation in short and long period mutants in which anticipated dawn does not match external dawn.

Unexpectedly, St0 did not correlate well with the shift in dawn transcript peak time in circadian clock mutants grown in a light-dark cycle (Fig. 9C-D). Although the correlation was maintained for *lhy cca1*, *toc1*, *gi* and *elf3*, there was a major discrepancy for *prp7 prp9*. In this long period mutant, starch degradation was strongly delayed (St0 > 5 h) even though in a light-dark cycle the *LHY* and *CCA1* transcripts peaked at a similar time in *prp7 prp9* and wild-type Col-0. Comparison of the temporal dynamics of circadian clock transcripts in *prp7 prp9* in LD and continuous light provided an explanation for this discrepancy. In the first part of the 24 h cycle, transcripts in *prp7 prp9* showed a similar response in light-dark cycles and continuous light. In both light regimes, *LHY* and *CCA1* transcripts remained high for many hours instead of declining rapidly as they do in wild-type plants. However, dusk and evening clock transcripts in *prp7 prp9* responded differently in continuous light and light-dark cycles. Whereas in continuous light they decayed slowly, resulting in a strong delay in the rise of the *LHY* and *CCA1* transcripts, in light-dark cycles the dusk and evening transcripts decayed rapidly after darkening, explaining why *LHY* and *CCA1* transcripts rose before dawn as in wild-type plants (Fig. 9E-G). These observations indicate that starch degradation is regulated by an output that is generated early in the 24 h clock cycle, when circadian clock progression is delayed in *prp7 prp9*, and subsequently operates independently of changes in circadian clock progression.

The rate of starch mobilization increases progressively across a wide range of photoperiods, ranging from 4 to 18 h (Gibon *et al.* 2009; Sulpice *et al.* 2014b), implying that the circadian clock can set an appropriate rate of starch mobilization over most of the 24 h cycle. Further, starch mobilization is immediately slowed in response to an early dusk (Graf *et al.* 2010), and is accelerated after a late dusk or interrupting the night with light for a short time (Scialdone *et al.* 2013). These responses are explained by a model in which early in the 24 h cycle the circadian clock activates a Timer that decays slowly during the rest of the 24 h (see above). In

principle, decay of the putative Timer might be continuously coupled to the circadian clock, or might become uncoupled from further progression of the clock through its cycle (Seaton *et al.* 2014). The relatively robust response of starch turnover in five circadian clock mutants in our study and in particular the pattern in *prp7 prp9* is consistent with model variants 2 and 3 from Seaton *et al.* (2014), in which an integrated output from the circadian clock sets a Timer that then becomes uncoupled from the clock.

Our observations are consistent with a model in which setting of the Timer is inhibited by dawn components and promoted by dusk and/or evening components (Supplemental Fig. S15). To accommodate this interaction, it seems likely that the Timer is reset 'X' hours after dawn, and runs down in '24-X' hours. Premature exhaustion of starch in *lhy cca1* is explained because the Timer is reset too early, and incomplete use of starch in *toc1*, *gi* and *elf3* is explained by a delay in resetting of the Timer. The incomplete use of starch in *prp7 prp9* is explained because *CCA1* and *LHY* expression remain high and dusk and evening gene expression does not rise until later in the T-cycle, which will delay resetting of the Timer. Interacting negative and positive outputs may provide greater robustness and sensitivity, for example, antagonistic action of dawn and dusk/evening components would explain why mutants with lesions in single circadian clock components can still adjust the rate of degradation after an early dusk. It is not necessary that *TOC1*, *GI* and *ELF3* all act as activators; for example, the delay in the exhaustion of starch in *gi* could be explained by a slower decline of the dawn genes or delayed rise of the evening genes in this mutant. It is also possible that other circadian clock associated genes are involved, for example *TIC*, which has a starch excess phenotype, is proposed to act at dawn, and has an earlier peak of expression of *GI* transcript and a delayed peak of expression of *ELF3* in light-dark conditions (Hall *et al.* 2003; Ding *et al.* 2007; Sanchez-Villarreal *et al.* 2013).

Further experiments will be required to discover the molecular identity of the Timer. Although there are marked diel rhythms in transcripts for starch-degrading enzymes (Smith *et al.* 2004; Blasing 2005; Flis *et al.* 2016), they are not accompanied by rapid changes in the abundance of the encoded proteins (Smith *et al.* 2004; Lu *et al.* 2005; Skeffington *et al.* 2014). Even BAM3 protein, which has relatively rapid half-life of 0.43 days (Li *et al.* 2017) would require 10 h for protein abundance to be halved after completely stopping BAM3 synthesis. The mechanism is more likely to involve synthesis and slow decay of a regulatory protein or slow reversion of a posttranslational modification.

Overall, our results show that starch mobilization is paced to dawn by a redundant and highly buffered network. That said, starch phenotypes of circadian clock and related mutants may not always be directly related to the mechanism that paces mobilization to dawn. Starch phenotypes in *gi* (Rédei 1962; Eimert *et al.* 1995; Messerli *et al.* 2007), *tic* (Sanchez-Villarreal *et al.* 2013), and *prp5 prp7 prp9* (Ruts *et al.* 2012) may reflect incomplete mobilization. In *gi*, incomplete use of starch accompanied by elevated levels of many sugars and organic acids (Messerli *et al.* 2007). A similar trend was visible in our experiments, although less marked, possibly reflecting differing growth conditions in the two studies. These results indicate that starch degradation in *gi* may be limited by low demand for C. Accumulation of sugars leads to a rise of trehalose 6-phosphate and feedback inhibition of starch degradation (Martins *et al.* 2013; Lunn *et al.* 2014). In *tic*, incomplete starch mobilization might be due to defects in C-sensing or a secondary consequence of the activation of stress responses (Sanchez-Villarreal *et al.* 2013). The latter might also contribute to incomplete turnover in *prp5 prp7 prp9* (Nakamichi *et al.* 2009). More generally, mutants with strongly impaired growth are likely to accumulate starch due to lack of demand.

### **Premature exhaustion of starch in *lhy cca1* leads to transient starvation**

Premature exhaustion of starch has a major impact on metabolism. At dawn, compared to wild-type plants or other circadian clock mutants, *lhy cca1* has low levels of sugars, phosphorylated intermediates and the sucrose-signal Tre6P, and high levels of Asn and many minor amino acids (Fig. 4; Supplemental Figs S6-7, Table 1). This metabolic phenotype resembles the night-time phenotype of the starchless *pgm* mutant, or the response of wild-type plants to a short extension of the night (Thimm *et al.* 2004; Gibon *et al.* 2006; Usadel *et al.* 2008). Minor amino acids typically increase in C-starvation as a result of protein catabolism (Izumi *et al.* 2013; Pilkington *et al.* 2014).

C starvation has been reported to influence the clock via several routes including stabilization of GI (Dalchau *et al.* 2011; Haydon *et al.* 2017) and induction of *PRR7* (Haydon *et al.* 2013). SnRK1 plays a major role in C-starvation signaling (Toroser *et al.* 2000; Zhang *et al.* 2009; Baena-González 2010; Nunes *et al.* 2013). It was recently reported that SnRK1 overexpression leads to changes in clock periodicity that are dependent on *TIC* (Shin *et al.* 2017). Transient C-starvation at the end of the night in *lhy cca1* may activate SnRK1 and contribute to the strong expression of *PRR7* in *lhy cca1*. Wild-type plants, however, pace mobilization to dawn over a wide range of growth conditions and in the face of sudden

perturbations and this will minimize the risk of C starvation (see Introduction, also Suppl Fig. S12). C starvation-related inputs probably only play a major role when an extreme combination of factors leads to a major shortfall in starch.

### **Circadian oscillation of the central intermediate glucose 6-phosphate**

A further striking metabolic phenotype was the strong oscillation in Glc6P levels in continuous light. This oscillation was seen in all mutants, with a trend for the period to be shorter in the short period mutant *lhy cca1*, and longer in the long period mutant *prp7 prp9*. Glc6P is a product of photosynthesis and starch degradation, a precursor for starch and sucrose synthesis, and the starting point for glycolysis, respiration and the biosynthesis of precursors for structural cellular components. The oscillation reveals that circadian regulation shifts the balance between Glc6P formation and consumption to favor Glc6P utilization in the subjective day and Glc6P formation during the subjective night.

The rise in Glc6P was accompanied by a weak peak of glucose and fructose, and coincided with the time at which starch accumulation plateaued (Figs 4B, 5D; Supplemental Fig. S3E).

We recently reported an explanation for the plateauing of starch accumulation upon transfer to continuous light (see Supplemental Fig. S3A). We found that starch degradation in the light is negligible early in the 24 h cycle, but rises progressively from around ZT12-14 (Fernandez *et al.* 2017). This results in a cycle of starch synthesis and degradation, which progressively decreases the net rate of starch accumulation. The cycle explains the oscillation in Glc6P in continuous light. In the subjective day assimilated C is partitioned between starch synthesis and sucrose synthesis whereas in the subjective night assimilation continues but the C supply increases because C is additionally available from starch degradation, driving Glc6P up.

In a light-dark cycle, the circadian oscillation of Glc6P is modified by direct responses to light and darkness. Photosynthesis would be expected to increase formation of Glc6P. Somewhat surprisingly Glc6P fell rapidly and strongly after the onset of illumination and rose rapidly and strongly after darkening (Figs. 4B, 5D, Supplemental Fig. S3E). In an earlier study, in which wild-type *Arabidopsis* was grown in different photoperiods, Glc6P increased after darkening, independently of time from dawn (Sulpice *et al.* 2014b), indicating that light directly or indirectly stimulates Glc6P consumption. Indeed, it is known that the use of Glc6P for sucrose, organic acid and amino acid synthesis is stimulated by light-, SnRK1- and Tre6P-dependent post-translational activation of enzymes like sucrose phosphate synthase (Huber &

Huber 1996; Huber *et al.* 2002), NR (Kaiser & Huber 2001; Huber *et al.* 2002; Lillo *et al.* 2004) and PEP carboxylase (Figueroa *et al.* 2016). It can be envisaged that in a light-dark cycle, circadian regulation and direct and indirect light regulation combine to increase Glc6P consumption for growth and reserve formation in the daytime, and to increase Glc6P release from reserves and decrease Glc6P utilization at night. This will poise metabolism to cope with the additional source of Glc6P provided by photosynthesis in the daytime.

### **Positive regulation of organic acid and N metabolism by dawn components**

Organic acids and amino acids are accumulated in the light to support energy metabolism and protein synthesis at night (Chia *et al.* 2000; Scheible *et al.* 2000; Urbanczyk-Wochniak *et al.* 2005; Fritz *et al.* 2006a; 2006b; Fahnenstich *et al.* 2007; Sulpice *et al.* 2014; Lehmann *et al.* 2015). In *Arabidopsis* the amount of C in organic acids is low relative to that in starch (Sulpice *et al.* 2014b). However, amino acids are an important reserve of reduced N (Piques *et al.* 2009; Pal *et al.* 2013). Per unit of N, nitrate reduction requires as much energy as the subsequent conversion of amino acids to protein (Penning De Vries 1975). Accumulation of amino acids in the light therefore greatly decreases the cost of protein synthesis in the night, when metabolism and growth is anyway constrained by the amount of starch accumulated in preceding light period.

Our results show that the circadian clock regulates diel organic acid and amino acid metabolism. Malate, fumarate and total amino acid levels oscillated in continuous light (Fig. 4C-D, Supplemental Fig. S3F-H) confirming earlier findings for individual amino acids (Espinoza *et al.* 2010). The period of these oscillations depended on clock period, being shorter in *lhy cca1* and longer in *prp7 prp9* (Fig. 4C-D). Furthermore, there were opposed responses in *lhy cca1* and *prp7 prp9*, with *lhy cca1* having low levels of many organic acids including malate, fumarate, citrate, isocitrate and aconitate between ZT6 and ZT16, and *prp7 prp9* having high levels of these metabolites (Figs 4C-D, 6C, Table 1, Supplemental Figs S3, S6). Many major and minor amino acids were present at low levels in *lhy cca1* and high levels in *prp7 prp9* (Supplemental Fig. S7). These differences were not a secondary effect due to changes in starch turnover; they occurred in the middle of the T-cycle when starch levels were high in both mutants, they were maintained in continuous light (Fig. 4D, Supplemental Fig. S3H), and *lhy cca1* still contained low organic acids and amino acids in a T-17 cycle when starch reserves lasted until dawn (Fig. 10, Supplemental Fig. S14).



Fukushima *et al.* (2009) reported high levels of organic acids and some amino acids in *prp5 prp7 prp9* mutants and a smaller elevation of organic acids in *CCA1*-overexpressers. Sanchez-Villarreal *et al.* (2013) reported modified levels of amino acids in the *tic* mutant, with higher levels of non-polar amino acids and fumarate and lower levels of N-rich amino acids. Possible reasons for these changes include activation of the TCA cycle (Fukushima *et al.* 2009) and changes in C-sensing or stress responses (Sanchez-Villarreal *et al.* 2013). However, interpretation might be complicated by large pleiotropic changes, including very slow growth and constitutive stress responses in *prp5 prp7 prp9* (Nakamichi *et al.* 2009) and strong stress responses in *tic1* (Sanchez-Villarreal *et al.* 2013).

Our analyses used a wider set of less strongly affected circadian mutants and included parallel analysis of circadian clock transcript dynamics. The simplest explanation for our results is that organic acid and amino acid metabolism is positively regulated by the dawn components. This explains the low levels of organic acid and amino acids in *lhy cca1* and the high levels in *prp7 prp9*, where *LHY* and *CCA1* transcripts remain high until the end of the light period (Flis *et al.* 2015; Supplemental Fig. S9). A direct role for the day components is unlikely because *PRR7* and *PRR9* function was abolished in *prp7 prp9*, and both transcripts declined early in the light period in *lhy cca1* (Flis *et al.* 2015; Supplemental Fig. S9). Multivariate analysis also identified a strong correlation between *LHY* and *CCA1* transcript abundance and malate and fumarate levels (Fig. 7A-B, Fig. 8C; Supplemental Fig. 11B). Whilst further research is required to identify the mechanisms by which the dawn components act, our results indicate that they include activation of nitrate reductase (Fig. 11).

Positive regulation of N metabolism by *LHY* and *CCA1* may provide a mechanism to balance N and C metabolism. Gutierrez *et al.* (2008) identified *CCA1* as a hub in an expression network. *CCA1* was positively correlated with *GLUTAMINE SYNTHASE 1*, but was also negatively correlated with *GLUTAMATE DEHYDROGENASE 1* and the transcription factor *bZIP1*, a positive regulator of *ASPARAGINE SYNTHASE 1*, *GLUTAMATE DEHYDROGENASE 1* and *bZIP1*, which are involved in C starvation responses. This reciprocal relationship points to *CCA1* being involved in balancing N and C metabolism. It is likely that *LHY* shows similar relationships, as expression of *CCA1* and *LHY* is tightly correlated (see Flis *et al.* 2015). As already mentioned, *PRR7* is induced by C starvation (Haydon *et al.* 2013), and our multivariate analyses revealed a negative relationship between *PRR7* transcript and sugars (Figs 7B-C, 8B). After induction by low sugar, *PRR7* represses *CCA1* and *LHY* (Haydon *et al.*, 2013). Our study reveals that the latter is likely to restrict

synthesis of organic acids and amino acids in the following light period. Up to now, coordination of C and N metabolism has been viewed in terms of interactions between C and N signaling and transcription and post-translational regulation of enzymes in central metabolism (Nunes-Nesi *et al.* 2010; Figueroa *et al.* 2016). These may be complemented by a circadian clock-mediated loop, which uses information about C status in the previous 24-h cycle to rebalance C and N metabolism in the coming cycle.

### Further metabolic phenotypes

Our study points to circadian regulation of further processes in central metabolism, in addition to diel turnover of C and N reserves. For example, whereas most amino acids were high at dusk in *prp7 prp9*, aromatic amino acids (Phe, Trp, Tyr) were lower than in other genotypes (Supplemental Fig. S7O-Q). As shikimate levels remained high in *prp7 prp9*, this may point to increased utilization for synthesis of phenylpropanoids. *lhy cca1* showed a particularly large decrease of Met, Cys and cystathionine at the end of the day compared to other genotypes (Supplemental Fig. S7T-V) indicating that dawn components regulate aspects of sulfur metabolism. A negative correlation of *ELF4* to *LHY*, *CCA1* and *PRR9*, and to malate, fumarate, glucose and fructose in the PC analysis indicated *ELF4* counteracts action of dawn components on these metabolites. Further, CC analysis pointed to interactions between *PRR5*, *GI* and N metabolism.

In conclusion, diel metabolism is regulated by multiple circadian clock outputs (summarized in Fig. 12). One, probably involving *ELF3*, is required for full rates of starch accumulation. A second involving *ELF3* regulates reducing sugar levels in the first part of the 24 h cycle. A third output, probably generated by an interaction between dawn and dusk or evening components, paces starch degradation to dawn. A fourth, possibly related, output favors Glc6P consumption in the light period and formation at night, buffering metabolism against the larger inflow of C from photosynthesis in the light period. A fifth output, in which the dawn components play a major role, regulates the synthesis of organic acids and build-up of amino acid reserves to support protein synthesis at night. Whilst these outputs can be dissected in mutants, in wild-type plants the clock is highly integrated and redundant, and the outputs that it generates are highly intertwined. This redundancy may be important in poising metabolism and resource allocation in fluctuating environments.

**Acknowledgements.** Research was supported by the Max Planck Society and European Union (FP7 collaborative project TiMet (contract no. 245143), by the Biotechnology and Biological Sciences Research Council (UK) in the form of an Institute Strategic Grant (BB/J004596/1) to the John Innes Centre, and by the John Innes Foundation. We are grateful to Karen Halliday for discussions about the EC-independent function of ELF3.

## Literature

- Amthor J.S. (2000) The McCree–de Wit–Penning de Vries–Thornley respiration paradigms: 30 years later. *Annals of Botany* **86**, 1–20.
- Apelt F., Breuer D., Nikoloski Z., Stitt M. & Kragler F. (2015) Phytotyping4D: A light-field imaging system for non-invasive and accurate monitoring of spatio-temporal plant growth. *The Plant Journal* **82**, 693–706.
- Apelt F., Breuer D., Olas J.J., Annunziata M.G., Flis A., Nikoloski Z., ... Stitt M. (2017) Circadian, carbon, and light control of expansion growth and leaf movement. *Plant Physiology* **174**, 1949–1968.
- Arrivault S., Guenther M., Ivakov A., Feil R., Vosloh D., Van Dongen J.T., ... Stitt M. (2009) Use of reverse-phase liquid chromatography, linked to tandem mass spectrometry, to profile the Calvin cycle and other metabolic intermediates in *Arabidopsis* rosettes at different carbon dioxide concentrations. *The Plant Journal* **59**, 824–839.
- Baena-González E. (2010) Energy signaling in the regulation of gene expression during stress. *Molecular Plant* **3**, 300–313.
- Baerenfaller K., Massonnet C., Walsh S., Baginsky S., Bühlmann P., Hennig L., ... Gruissem W. (2012) Systems-based analysis of *Arabidopsis* leaf growth reveals adaptation to water deficit. *Molecular Systems Biology* **8**, 606.
- Blasing O.E. (2005) Sugars and circadian regulation make major contributions to the global regulation of diurnal gene expression in *Arabidopsis*. *The Plant Cell* **17**, 3257–3281.
- Bradford M.M. (1976) A rapid and sensitive method for the quantitation of microgram quantities of protein utilizing the principle of protein-dye binding. *Analytical Biochemistry* **72**, 248–254.
- Britto D.T. & Kronzucker H.J. (2005) Nitrogen acquisition, PEP carboxylase, and cellular pH homeostasis: new views on old paradigms. *Plant, Cell & Environment* **28**, 1396–1409.
- Campbell W.H. (1999) Nitrate reductase structure, function and regulation: Bridging the gap between biochemistry and physiology. *Annual Review of Plant Physiology and Plant Molecular Biology* **50**, 277–303.

- Carré I. & Veflingstad S.R. (2013) Emerging design principles in the *Arabidopsis* circadian clock. *Seminars in Cell & Developmental Biology* **24**, 393–398.
- Caspar T., Huber S.C. & Somerville C. (1985) Alterations in growth, photosynthesis, and respiration in a starchless mutant of *Arabidopsis thaliana* (L.) deficient in chloroplast phosphoglucomutase activity. *Plant Physiology* **79**, 11–17.
- Chew Y.H., Seaton D.D., Mengin V., Flis A., Mugford S.T., Smith A.M., ... Millar A.J. (2017) Linking circadian time to growth rate quantitatively via carbon metabolism. *bioRxiv*, 105437.
- Chia D.W., Yoder T.J., Reiter W.-D. & Gibson S.I. (2000) Fumaric acid: An overlooked form of fixed carbon in *Arabidopsis* and other plant species. *Planta* **211**, 743–751.
- Coruzzi G.M. & Zhou L. (2001) Carbon and nitrogen sensing and signaling in plants: emerging ‘matrix effects.’ *Current Opinion in Plant Biology* **4**, 247–253.
- Covington M.F., Panda S., Liu X.L., Strayer C.A., Wagner D.R. & Kay S.A. (2001) ELF3 modulates resetting of the circadian clock in *Arabidopsis*. *The Plant Cell* **13**, 1305–1315.
- Cross J.M., von Korff M., Altmann T., Bartzetko L., Sulpice R., Gibon Y., ... Stitt M. (2006) Variation of enzyme activities and metabolite levels in 24 *Arabidopsis* accessions growing in carbon-limited conditions. *Plant Physiology* **142**, 1574–1588.
- Dalchau N., Baek S.J., Briggs H.M., Robertson F.C., Dodd A.N., Gardner M.J., ... Webb A.A.R. (2011) The circadian oscillator gene GIGANTEA mediates a long-term response of the *Arabidopsis thaliana* circadian clock to sucrose. *Proceedings of the National Academy of Sciences* **108**, 5104–5109.
- Deng X.W., Caspar T. & Quail P.H. (1991) *cop1*: a regulatory locus involved in light-controlled development and gene expression in *Arabidopsis*. *Genes & Development* **5**, 1172–1182.
- Ding Z., Millar A.J., Davis A.M. & Davis S.J. (2007) *TIME FOR COFFEE* encodes a nuclear regulator in the *Arabidopsis thaliana* circadian clock. *The Plant Cell* **19**, 1522–1536.
- Dixon L.E., Knox K., Kozma-Bognar L., Southern M.M., Pokhilko A. & Millar A.J. (2011) Temporal repression of core circadian genes is mediated through EARLY

FLOWERING 3 in Arabidopsis. *Current Biology* **21**, 120–125.

Dodd A.N., Belbin F.E., Frank A. & Webb A.A.R. (2015) Interactions between circadian clocks and photosynthesis for the temporal and spatial coordination of metabolism.

*Frontiers in Plant Science* **6**, 245.

Dodd A.N., Salathia N., Hall A., Kévei E., Tóth R., Nagy F., ... Webb A.A.R. (2005) Plant circadian clocks increase photosynthesis, growth, survival, and competitive advantage.

*Science* **309**, 630–633.

Dong G. & Golden S.S. (2008) How a cyanobacterium tells time. *Current Opinion in Microbiology* **11**, 541–546.

Dornbusch T., Michaud O., Xenarios I. & Fankhauser C. (2014) Differentially phased leaf growth and movements in Arabidopsis depend on coordinated circadian and light regulation. *The Plant Cell* **26**, 3911–3921.

Edwards K.D., Akman O.E., Knox K., Lumsden P.J., Thomson A.W., Brown P.E., ... Millar A.J. (2010) Quantitative analysis of regulatory flexibility under changing environmental conditions. *Molecular Systems Biology* **6**, 1–11.

Eimert K., Wang S.M., Lue W.I. & Chen J. (1995) Monogenic recessive mutations causing both late floral initiation and excess starch accumulation in Arabidopsis. *The Plant Cell* **7**, 1703–1712.

Espinoza C., Degenkolbe T., Caldana C., Zuther E., Leisse A., Willmitzer L., ... Hannah M.A. (2010) Interaction with diurnal and circadian regulation results in dynamic metabolic and transcriptional changes during cold acclimation in Arabidopsis. *PLoS One* **5**, e14101.

Fahnenstich H., Saigo M., Niessen M., Zanol M.I., Andreo C.S., Fernie A.R., ... Maurino V.G. (2007) Alteration of organic acid metabolism in Arabidopsis overexpressing the maize C4 NADP-malic enzyme causes accelerated senescence during extended darkness. *Plant physiology* **145**, 640–652.

Farré E.M. & Weise S.E. (2012) The interactions between the circadian clock and primary metabolism. *Current Opinion in Plant Biology* **15**, 293–300.

Fernandez O., Ishihara H., George G.M., Mengin V., Flis A., Sumner D., ... Stitt M. (2017)



- Foliar starch turnover occurs in long days and in falling light at the end of the day. *Plant Physiology* **44**, pp.00601.2017.
- Figueroa C.M., Feil R., Ishihara H., Watanabe M., Kölling K., Krause U., ... Lunn J.E. (2016) Trehalose 6-phosphate coordinates organic and amino acid metabolism with carbon availability. *The Plant Journal* **85**, 410–423.
- Flis A., Piñas Fernández A., Zielinski T., Mengin V., Sulpice R., Stratford K., ... Millar A.J. (2015) Defining the robust behaviour of the plant clock gene circuit with absolute RNA timeseries and open infrastructure. *Open Biology* **5**, 1–21.
- Flis A., Sulpice R., Seaton D.D., Ivakov A.A., Liput M., Abel C., ... Stitt M. (2016) Photoperiod-dependent changes in the phase of core clock transcripts and global transcriptional outputs at dawn and dusk in Arabidopsis. *Plant, Cell & Environment* **39**, 1955–1981.
- Fogelmark K. & Troein C. (2014) Rethinking transcriptional activation in the Arabidopsis circadian clock. *PLoS Computational Biology* **10**, e1003705.
- Fritz C., Mueller C., Matt P., Feil R. & Stitt M. (2006a) Impact of the C-N status on the amino acid profile in tobacco source leaves. *Plant, Cell & Environment* **29**, 2055–2076.
- Fritz C., Palacios-Rojas N., Feil R. & Stitt M. (2006b) Regulation of secondary metabolism by the carbon-nitrogen status in tobacco: nitrate inhibits large sectors of phenylpropanoid metabolism. *The Plant Journal* **46**, 533–548.
- Fukushima A., Kusano M., Nakamichi N., Kobayashi M., Hayashi N., Sakakibara H., ... Saito K. (2009) Impact of clock-associated Arabidopsis pseudo-response regulators in metabolic coordination. *Proceedings of the National Academy of Sciences* **106**, 7251–7256.
- Gibon Y., Bläsing O.E., Hannemann J., Carillo P., Höhne M., Hendriks J.H.M., ... Stitt M. (2004a) A robot-based platform to measure multiple enzyme activities in Arabidopsis using a set of cycling assays: comparison of changes of enzyme activities and transcript levels during diurnal cycles and in prolonged darkness. *The Plant Cell* **16**, 3304–3325.
- Gibon Y., Bläsing O.E., Palacios-Rojas N., Pankovic D., Hendriks J.H.M., Fisahn J., ... Stitt M. (2004b) Adjustment of diurnal starch turnover to short days: depletion of sugar

during the night leads to a temporary inhibition of carbohydrate utilization, accumulation of sugars and post-translational activation of ADP-glucose pyrophosphorylase in the following a light period. *The Plant Journal* **39**, 847–862.

Gibon Y., Pyl E.-T., Sulpice R., Lunn J.E., Höhne M., Günther M. & Stitt M. (2009) Adjustment of growth, starch turnover, protein content and central metabolism to a decrease of the carbon supply when *Arabidopsis* is grown in very short photoperiods. *Plant, Cell & Environment* **32**, 859–874.

Gibon Y., Usadel B., Blaesing O.E., Kamlage B., Hoehne M., Trethewey R. & Stitt M. (2006) Integration of metabolite with transcript and enzyme activity profiling during diurnal cycles in *Arabidopsis* rosettes. *Genome Biology* **7**, R76.

Graf A., Schlereth A., Stitt M. & Smith A.M. (2010) Circadian control of carbohydrate availability for growth in *Arabidopsis* plants at night. *Proceedings of the National Academy of Sciences* **107**, 9458–9463.

Graf A. & Smith A.M. (2011) Starch and the clock: the dark side of plant productivity. *Trends in Plant Science* **16**, 169–175.

Greenham K. & McClung C.R. (2015) Integrating circadian dynamics with physiological processes in plants. *Nature Reviews Genetics* **16**, 598–610.

Gutierrez R.A., Stokes T.L., Thum K., Xu X., Obertello M., Katari M.S., ... Coruzzi G.M. (2008) Systems approach identifies an organic nitrogen-responsive gene network that is regulated by the master clock control gene CCA1. *Proceedings of the National Academy of Sciences* **105**, 4939–4944.

Hall A., Bastow R.M., Davis S.J., Hanano S., Mewatters H.G., Hibberd V., ... Millar A.J. (2003) The *TIME FOR COFFEE* gene maintains the amplitude and timing of *Arabidopsis* circadian clocks. *The Plant Cell* **15**, 2719–2729.

Harmer S.L. (2009) The circadian system in higher plants. *Annual Review of Plant Biology* **60**, 357–377.

Harmer S.L., Hogenesch J.B., Straume M., Chang H.-S.S., Han B., Zhu T., ... Kay S.A. (2000) Orchestrated transcription of key pathways in *Arabidopsis* by the circadian clock. *Science* **290**, 2110–2113.

- Harmer S.L., Panda S. & Kay S.A. (2001) Molecular bases of circadian rhythms. *Annual Review of Cell and Developmental Biology* **17**, 215–253.
- Haydon M.J., Mielczarek O., Frank A., Román Á. & Webb A.A. (2017) Sucrose and ethylene signaling interact to modulate the circadian clock. *Plant Physiology* **175**, 947–958.
- Haydon M.J., Mielczarek O., Robertson F.C., Hubbard K.E. & Webb A.A.R. (2013) Photosynthetic entrainment of the *Arabidopsis thaliana* circadian clock. *Nature* **502**, 689–692.
- Helfer A., Nusinow D.A., Chow B.Y., Gehrke A.R., Bulyk M.L. & Kay S.A. (2011) LUX ARRHYTHMO encodes a nighttime repressor of circadian gene expression in the Arabidopsis core clock. *Current Biology* **21**, 126–133.
- Herrero E., Kolmos E., Bujdoso N., Yuan Y., Wang M., Berns M.C., ... Davis S.J. (2012) *EARLY FLOWERING4* recruitment of *EARLY FLOWERING3* in the nucleus sustains the Arabidopsis circadian clock. *The Plant Cell* **24**, 428–443.
- Hicks K.A., Millar A.J., Carre I.A., Somers D.E., Straume M., Meeks-Wagner D.R. & Kay S.A. (1996) Conditional circadian dysfunction of the Arabidopsis *early-flowering 3* mutant. *Science* **274**, 790–792.
- Hornitschek P., Kohnen M. V., Lorrain S., Rougemont J., Ljung K., López-Vidriero I., ... Fankhauser C. (2012) Phytochrome interacting factors 4 and 5 control seedling growth in changing light conditions by directly controlling auxin signaling. *The Plant Journal* **71**, 699–711.
- Hotelling H. (1936) Relations between two sets of variates. *Biometrika* **28**, 321.
- Hsu P.Y., Devisetty U.K. & Harmer S.L. (2013) Accurate timekeeping is controlled by a cycling activator in Arabidopsis. *eLife* **2**, e00473.
- Huber S.C. & Huber J.L. (1996) Role and regulation of sucrose-phosphate synthase in higher plants. *Annual Review of Plant Physiology and Plant Molecular Biology* **47**, 431–444.
- Huber S.C., MacKintosh C. & Kaiser W.M. (2002) Metabolic enzymes as targets for 14-3-3 proteins. *Plant Molecular Biology* **50**, 1053–1063.
- Ishihara H., Obata T., Sulpice R., Fernie A.R. & Stitt M. (2015) Quantifying protein

synthesis and degradation in Arabidopsis by dynamic  $^{13}\text{CO}_2$  labeling and analysis of enrichment in individual amino acids in their free pools and in protein. *Plant Physiology* **168**, 74–93.

Izumi M., Hidema J., Makino A. & Ishida H. (2013) Autophagy contributes to nighttime energy availability for growth in Arabidopsis. *Plant Physiology* **161**, 1682–1693.

Johnson C.H., Elliott J.A. & Foster R. (2003) Entrainment of circadian programs. *Chronobiology International* **20**, 741–774.

Kaiser W.M. & Huber S.C. (2001) Post-translational regulation of nitrate reductase: mechanism, physiological relevance and environmental triggers. *Journal of Experimental Botany* **52**, 1981–1989.

Kinmonth-Schultz H.A., Golembeski G.S. & Imaizumi T. (2013) Circadian clock-regulated physiological outputs: dynamic responses in nature. *Seminars in Cell & Developmental Biology* **24**, 407–413.

Lehmann M.M., Rinne K.T., Blessing C., Siegwolf R.T.W., Buchmann N. & Werner R.A. (2015) Malate as a key carbon source of leaf dark-respired  $\text{CO}_2$  across different environmental conditions in potato plants. *Journal of Experimental Botany* **66**, 5769–5781.

Li J., Zhou W., Francisco P., Wong R., Zhang D. & Smith S.M. (2017) Inhibition of Arabidopsis chloroplast  $\beta$ -amylase BAM3 by maltotriose suggests a mechanism for the control of transitory leaf starch mobilisation. *PloS One* **12**, e0172504.

Lillo C., Meyer C., Lea U.S., Provan F. & Oltedal S. (2004) Mechanism and importance of post-translational regulation of nitrate reductase. *Journal of Experimental Botany* **55**, 1275–1282.

Lillo C., Meyer C. & Ruoff P. (2001) The nitrate reductase circadian system. The central clock dogma contra multiple oscillatory feedback loops. *Plant Physiology* **125**, 1554–1557.

Lu Y., Gehan J.P. & Sharkey T.D. (2005) Daylength and circadian effects on starch degradation and maltose metabolism. *Plant Physiology* **138**, 2280–2291.

Lunn J.E., Delorge I., Figueroa C.M., Van Dijck P. & Stitt M. (2014) Trehalose metabolism

in plants. *The Plant Journal* **79**, 544–567.

Lunn J.E., Feil R., Hendriks J.H.M., Gibon Y., Morcuende R., Osuna D., ... Stitt M. (2006) Sugar-induced increases in trehalose 6-phosphate are correlated with redox activation of ADPglucose pyrophosphorylase and higher rates of starch synthesis in *Arabidopsis thaliana*. *Biochemical Journal* **397**, 139–148.

Martin-Tryon E.L., Kreps J.A. & Harmer S.L. (2007) *GIGANTEA* acts in blue light signaling and has biochemically separable roles in circadian clock and flowering time regulation. *Plant Physiology* **143**, 473–486.

Martins M.C.M., Hejazi M., Fettke J., Steup M., Feil R., Krause U., ... Lunn J.E. (2013) Feedback inhibition of starch degradation in *Arabidopsis* leaves mediated by trehalose 6-phosphate. *Plant Physiology* **163**, 1142–1163.

Mengin V., Pyl E.-T., Alexandre Moraes T., Sulpice R., Krohn N., Encke B. & Stitt M. (2017) Photosynthate partitioning to starch in *Arabidopsis thaliana* is insensitive to light intensity but sensitive to photoperiod due to a restriction on growth in the light in short photoperiods. *Plant, Cell & Environment*, 2608–2627.

Messerli G., Partovi Nia V., Trevisan M., Kolbe A., Schauer N., Geigenberger P., ... Zeeman S.C. (2007) Rapid classification of phenotypic mutants of *Arabidopsis* via metabolite fingerprinting. *Plant Physiology* **143**, 1484–1492.

Michael T.P., Mockler T.C., Breton G., McEntee C., Byer A., Trout J.D., ... Chory J. (2008) Network discovery pipeline elucidates conserved time-of-day-specific cis-regulatory modules. *PLoS Genetics* **4**, e14.

Millar A.J. (2004) Input signals to the plant circadian clock. *Journal of Experimental Botany* **55**, 277–283.

Miller A.J., Fan X., Shen Q. & Smith S.J. (2007) Amino acids and nitrate as signals for the regulation of nitrogen acquisition. *Journal of Experimental Botany* **59**, 111–119.

Mizoguchi T., Wheatley K., Hanzawa Y., Wright L., Mizoguchi M., Song H.-R., ... Coupland G. (2002) *LHY* and *CCA1* are partially redundant genes required to maintain circadian rhythms in *Arabidopsis*. *Developmental Cell* **2**, 629–641.

Mizuno T., Nomoto Y., Oka H., Kitayama M., Takeuchi A., Tsubouchi M. & Yamashino T.

(2014) Ambient temperature signal feeds into the circadian clock transcriptional circuitry through the EC night-time repressor in *Arabidopsis thaliana*. *Plant & Cell Physiology* **55**, 958–76.

Mugford S.T., Fernandez O., Brinton J., Flis A., Krohn N., Encke B., ... Smith A.M. (2014) Regulatory properties of ADP glucose pyrophosphorylase are required for adjustment of leaf starch synthesis in different photoperiods. *Plant Physiology* **166**, 1733–1747.

Nakamichi N. (2011) Molecular mechanisms underlying the Arabidopsis circadian clock. *Plant & Cell Physiology* **52**, 1709–1718.

Nakamichi N., Kusano M., Fukushima A., Kita M., Ito S., Yamashino T., ... Mizuno T. (2009) Transcript profiling of an Arabidopsis *PSEUDO RESPONSE REGULATOR* arrhythmic triple mutant reveals a role for the circadian clock in cold stress response. *Plant and Cell Physiology* **50**, 447–462.

Nieto C., López-Salmerón V., Davière J.-M. & Prat S. (2015) ELF3-PIF4 interaction regulates plant growth independently of the evening complex. *Current Biology* **25**, 187–193.

Novitskaya L., Trevanion S.J., Driscoll S., Foyer C.H. & Noctor G. (2002) How does photorespiration modulate leaf amino acid contents? A dual approach through modelling and metabolite analysis. *Plant, Cell & Environment* **25**, 821–835.

Nozue K., Covington M.F., Duek P.D., Lorrain S., Fankhauser C., Harmer S.L. & Maloof J.N. (2007) Rhythmic growth explained by coincidence between internal and external cues. *Nature* **448**, 358–361.

Nunes-Nesi A., Carrari F., Gibon Y., Sulpice R., Lytovchenko A., Fisahn J., ... Fernie A.R. (2007) Deficiency of mitochondrial fumarase activity in tomato plants impairs photosynthesis via an effect on stomatal function. *The Plant Journal* **50**, 1093–1106.

Nunes-Nesi A., Fernie A.R. & Stitt M. (2010) Metabolic and signaling aspects underpinning the regulation of plant carbon nitrogen interactions. *Molecular plant* **3**, 973–996.

Nunes C., Primavesi L.F., Patel M.K., Martinez-Barajas E., Powers S.J., Sagar R., ... Paul M.J. (2013) Inhibition of SnRK1 by metabolites: Tissue-dependent effects and cooperative inhibition by glucose 1-phosphate in combination with trehalose 6-



phosphate. *Plant Physiology and Biochemistry* **63**, 89–98.

Nusinow D.A., Helfer A., Hamilton E.E., King J.J., Imaizumi T., Schultz T.F., ... Kay S.A. (2011) The ELF4-ELF3-LUX complex links the circadian clock to diurnal control of hypocotyl growth. *Nature* **475**, 398–402.

Pal S.K., Liput M., Piques M., Ishihara H., Obata T., Martins M.C.M., ... Stitt M. (2013) Diurnal changes of polysome loading track sucrose content in the rosette of wild-type *Arabidopsis* and the starchless *pgm* mutant. *Plant Physiology* **162**, 1246–1265.

Penning De Vries F.W.T. (1975) The cost of maintenance processes in plant cells. *Annals of Botany* **39**, 77–92.

Pilgrim M.L., Caspar T., Quail P.H. & McClung C.R. (1993) Circadian and light-regulated expression of nitrate reductase in *Arabidopsis*. *Plant Molecular Biology* **23**, 349–364.

Pilkington S.M., Encke B., Krohn N., Höhne M., Stitt M. & Pyl E.-T. (2014) Relationship between starch degradation and carbon demand for maintenance and growth in *Arabidopsis thaliana* in different irradiance and temperature regimes. *Plant, Cell & Environment* **38**, 157–171.

Piques M., Schulze W.X., Höhne M., Usadel B., Gibon Y., Rohwer J. & Stitt M. (2009) Ribosome and transcript copy numbers, polysome occupancy and enzyme dynamics in *Arabidopsis*. *Molecular Systems Biology* **5**, 1–17.

Poiré R., Wiese-Klinkenberg A., Parent B., Mielewczik M., Schurr U., Tardieu F. & Walter A. (2010) Diel time-courses of leaf growth in monocot and dicot species: endogenous rhythms and temperature effects. *Journal of Experimental Botany* **61**, 1751–1759.

Pokhilko A., Fernández A.P., Edwards K.D., Southern M.M., Halliday K.J. & Millar A.J. (2012) The clock gene circuit in *Arabidopsis* includes a repressilator with additional feedback loops. *Molecular Systems Biology* **8**, 1–13.

Pyl E.-T., Piques M., Ivakov A., Schulze W., Ishihara H., Stitt M. & Sulpice R. (2012) Metabolism and growth in *Arabidopsis* depend on the daytime temperature but are temperature-compensated against cool nights. *The Plant Cell* **24**, 2443–2469.

R Core Team (2017) R: A language and environment for statistical computing. *R Foundation for statistical computing*, <http://www.R-project.org/>.

- Raven J.A. (1986) Biochemical disposal of excess  $H^+$  in growing plants? *New Phytologist* **104**, 175–206.
- Rédei G.P. (1962) Supervital mutants of *Arabidopsis*. *Genetics* **47**, 443–60.
- Ruts T., Matsubara S., Wiese-Klinkenberg A. & Walter A. (2012) Aberrant temporal growth pattern and morphology of root and shoot caused by a defective circadian clock in *Arabidopsis thaliana*. *The Plant Journal* **72**, 154–161.
- Salomé P.A. & McClung C.R. (2005) *PSEUDO-RESPONSE REGULATOR 7* and *9* are partially redundant genes essential for the temperature responsiveness of the *Arabidopsis* circadian clock. *The Plant Cell* **17**, 791–803.
- Sanchez-Villarreal A., Shin J., Bujdoso N., Obata T., Neumann U., Du S.X., ... Davis S.J. (2013) TIME for COFFEE is an essential component in the maintenance of metabolic homeostasis in *Arabidopsis thaliana*. *The Plant Journal* **76**, 188–200.
- Scheible W.-R., Gonzalez-Fontes A., Lauerer M., Muller-Rober B., Caboche M. & Stitt M. (1997) Nitrate acts as a signal to induce organic acid metabolism and repress starch metabolism in tobacco. *The Plant Cell* **9**, 783–798.
- Scheible W.-R., Krapp A. & Stitt M. (2000) Reciprocal diurnal changes of phosphoenolpyruvate carboxylase expression and cytosolic pyruvate kinase, citrate synthase and NADP-isocitrate dehydrogenase expression regulate organic acid metabolism during nitrate assimilation in tobacco leaves. *Plant, Cell & Environment* **23**, 1155–1167.
- Scialdone A. & Howard M. (2015) How plants manage food reserves at night: quantitative models and open questions. *Frontiers in Plant Science* **6**, 204.
- Scialdone A., Mugford S.T., Feike D., Skeffington A., Borrill P., Graf A., ... Howard M. (2013) *Arabidopsis* plants perform arithmetic division to prevent starvation at night. *eLife* **2**, 1–24.
- Seaton D.D., Ebenhoh O., Millar A.J. & Pokhilko A. (2014) Regulatory principles and experimental approaches to the circadian control of starch turnover. *Journal of The Royal Society Interface* **11**, 20130979.
- Seaton D.D., Graf A., Baerenfaller K., Stitt M., Millar A.J. & Gruissem W. (2018)

Photoperiodic control of the Arabidopsis proteome reveals a translational coincidence mechanism. *Molecular Systems Biology* **14**, e7962.

Seaton D.D., Smith R.W., Song Y.H., MacGregor D.R., Stewart K., Steel G., ... Halliday K.J. (2015) Linked circadian outputs control elongation growth and flowering in response to photoperiod and temperature. *Molecular Systems Biology* **11**, 1–19.

Seo P.J. & Mas P. (2014) Multiple layers of posttranslational regulation refine circadian clock activity in Arabidopsis. *The Plant Cell* **26**, 79–87.

Shin J., Sánchez-Villarreal A., Davis A.M., Du S.X., Berendzen K.W., Koncz C., ... Davis S.J. (2017) The metabolic sensor AKIN10 modulates the Arabidopsis circadian clock in a light-dependent manner. *Plant Cell & Environment* **40**, 997–1008.

Skeffington A.W., Graf A., Duxbury Z., Gruissem W. & Smith A.M. (2014) Glucan, water dikinase exerts little control over starch degradation in Arabidopsis leaves at night. *Plant Physiology* **165**, 866–879.

Smith A.M. & Stitt M. (2007) Coordination of carbon supply and plant growth. *Plant, Cell & Environment* **30**, 1126–1149.

Smith S.M., Fulton D.C., Chia T., Thorneycroft D., Chapple A., Dunstan H.D., ... Smith A.M. (2004) Diurnal changes in the transcriptome encoding enzymes of starch metabolism provide evidence for both transcriptional and posttranscriptional regulation of starch metabolism in Arabidopsis leaves. *Plant Physiology* **136**, 2687–2699.

Somers D.E., Webb A.A.R., Pearson M. & Kay S.A. (1998) The short-period mutant, *toc1-1*, alters circadian clock regulation of multiple outputs throughout development in *Arabidopsis thaliana*. *Development* **125**, 485–494.

Song Y.H., Shim J.S., Kinmonth-Schultz H.A. & Imaizumi T. (2015) Photoperiodic flowering: time measurement mechanisms in leaves. *Annual Review of Plant Biology* **66**, 441–464.

Staiger D., Shin J., Johansson M. & Davis S.J. (2013) The circadian clock goes genomic. *Genome Biology* **14**, 1–8.

Stewart D. & Love W. (1968) A general canonical correlation index. *Psychological Bulletin* **70**, 160–163.

- Stitt M. & Gibon Y. (2014) Why measure enzyme activities in the era of systems biology? *Trends in Plant Science* **19**, 256–265.
- Stitt M. & Krapp A. (1999) The interaction between elevated carbon dioxide and nitrogen nutrition: the physiological and molecular background. *Plant, Cell & Environment* **22**, 553–621.
- Stitt M., Lunn J. & Usadel B. (2010) Arabidopsis and primary photosynthetic metabolism - more than the icing on the cake. *The Plant Journal* **61**, 1067–1091.
- Stitt M., Müller C., Matt P., Gibon Y., Carillo P., Morcuende R., ... Krapp A. (2002) Steps towards an integrated view of nitrogen metabolism. *Journal of Experimental Botany* **53**, 959–970.
- Stitt M. & Zeeman S.C. (2012) Starch turnover: pathways, regulation and role in growth. *Current Opinion in Plant Biology* **15**, 282–292.
- Sulpice R., Flis A., Ivakov A.A., Apelt F., Krohn N., Encke B., ... Stitt M. (2014a) Arabidopsis Coordinates the Diurnal Regulation of Carbon Allocation and Growth across a Wide Range of Photoperiods. **7**, 137–155.
- Sulpice R., Flis A., Ivakov A.A., Apelt F., Krohn N., Encke B., ... Stitt M. (2014b) Arabidopsis coordinates the diurnal regulation of carbon allocation and growth across a wide range of photoperiods. *Molecular Plant* **7**, 137–155.
- Thimm O., Bläsing O., Gibon Y., Nagel A., Meyer S., Krüger P., ... Stitt M. (2004) MAPMAN: a user-driven tool to display genomics data sets onto diagrams of metabolic pathways and other biological processes. *The Plant Journal* **37**, 914–939.
- Toroser D., Plaut Z. & Huber S.C. (2000) Regulation of a plant SNF1-Related Protein Kinase by glucose 6-phosphate. *Plant Physiology* **123**, 403–412.
- Trevanion S.J., Castleden C.K., Foyer C.H., Furbank R.T., Quick W.P. & Lunn J.E. (2004) Regulation of sucrose-phosphate synthase in wheat (*Triticum aestivum*) leaves. *Functional Plant Biology* **31**, 685–695.
- Urbanczyk-Wochniak E., Baxter C., Kolbe A., Kopka J., Sweetlove L.J. & Fernie A.R. (2005) Profiling of diurnal patterns of metabolite and transcript abundance in potato (*Solanum tuberosum*) leaves. *Planta* **221**, 891–903.

- Usadel B., Blasing O.E., Gibon Y., Retzlaff K., Hohne M., Gunther M. & Stitt M. (2008) Global transcript levels respond to small changes of the carbon status during progressive exhaustion of carbohydrates in *Arabidopsis* rosettes. *Plant Physiology* **146**, 1834–1861.
- Vincentz M., Moureaux T., Leydecker M.-T., Vaucheret H. & Caboche M. (1993) Regulation of nitrate and nitrite reductase expression in *Nicotiana plumbaginifolia* leaves by nitrogen and carbon metabolites. *The Plant Journal* **3**, 315–324.
- Watanabe M., Balazadeh S., Tohge T., Erban A., Giavalisco P., Kopka J., ... Hoefgen R. (2013) Comprehensive dissection of spatiotemporal metabolic shifts in primary, secondary, and lipid metabolism during developmental senescence in *Arabidopsis*. *Plant Physiology* **162**, 1290–1310.
- Yadav U.P., Ivakov A., Feil R., Duan G.Y., Walther D., Giavalisco P., ... Lunn J.E. (2014) The sucrose-trehalose 6-phosphate (Tre6P) nexus: specificity and mechanisms of sucrose signalling by Tre6P. *Journal of Experimental Botany* **65**, 1051–1068.
- Yazdanbakhsh N., Sulpice R., Graf A., Stitt M. & Fisahn J. (2011) Circadian control of root elongation and C partitioning in *Arabidopsis thaliana*. *Plant, Cell & Environment* **34**, 877–894.
- Zagotta M.T., Shannon S., Jacobs C. & Meeks-Wagner D.R. (1992) Early-flowering mutants of *Arabidopsis thaliana*. *Australian Journal of Plant Physiology* **19**, 411–418.
- Zhang E.E. & Kay S.A. (2010) Clocks not winding down: unravelling circadian networks. *Nature Reviews Molecular Cell Biology* **11**, 764–776.
- Zhang Y., Primavesi L.F., Jhurrea D., Andralojc P.J., Mitchell R.A.C., Powers S.J., ... Paul M.J. (2009) Inhibition of SNF1-Related Protein Kinase1 activity and regulation of metabolic pathways by trehalose 6-phosphate. *Plant Physiology* **149**, 1860–1871.

**Table 1.** Levels of selected metabolites at dawn and dusk in wild-type Col-0 and Ws-2 and *lhy cca1*, *prp7 prp9*, *toc1*, *gi* and *elf3* mutants measured by LC-MS/MS. The measurements were carried out in the material from the experiment of Figs 1-5. All mutants were grown for 21 days except for the separate experiment with Ws-2 and *elf3*, which was harvested after 13 days (plant age is indicated in the left hand column). Values indicate mean  $\pm$  S.E. Significance at  $p < 0.05$  is indicated. Mutants are grouped with the corresponding wild-type. Data for more metabolites are provided in Supplemental Data file S3.

Genotype	Time point	Tre6P nmol / g FW	Sucrose6P nmol / g FW	3-PGA nmol / g FW	Citrate nmol / g FW	Shikimate nmol / g FW	Glutamate nmol / g FW
21 days old							
Col0	EN	0.061 $\pm$ 0.012	0.415 $\pm$ 0.066	158 $\pm$ 27	6785 $\pm$ 1426	20.2 $\pm$ 2.0	2751 $\pm$ 58
	ED	0.267 $\pm$ 0.017	0.407 $\pm$ 0.065	267 $\pm$ 56	3181 $\pm$ 327	53.7 $\pm$ 2.3	3603 $\pm$ 72
<i>gi</i>	EN	0.062 $\pm$ 0.006	0.463 $\pm$ 0.064	155 $\pm$ 19	4160 $\pm$ 598	19.0 $\pm$ 2.1	3014 $\pm$ 36
	ED	0.316 $\pm$ 0.019	0.374 $\pm$ 0.013	219 $\pm$ 34	3158 $\pm$ 114	51.3 $\pm$ 2.1	3618 $\pm$ 290
<i>toc 1</i>	EN	0.068 $\pm$ 0.004	0.453 $\pm$ 0.028	173 $\pm$ 8	6026 $\pm$ 238	20.6 $\pm$ 1.0	<b>*3623 <math>\pm</math> 14</b>
	ED	<b>*0.330 <math>\pm</math> 0.024</b>	0.415 $\pm$ 0.007	<b>*275 <math>\pm</math> 14</b>	3232 $\pm$ 546	<b>*52.8 <math>\pm</math> 2.7</b>	3579 $\pm$ 85
<i>prp7 prp9</i>	EN	0.180 $\pm$ 0.077	0.512 $\pm$ 0.074	204 $\pm$ 15	6903 $\pm$ 1768	40.7 $\pm$ 9.5	<b>*4101 <math>\pm</math> 53</b>
	ED	0.305 $\pm$ 0.009	0.479 $\pm$ 0.038	383 $\pm$ 28	<b>*4824 <math>\pm</math> 425</b>	59.5 $\pm$ 2.3	3474 $\pm$ 29
21 days old							
Ws2	EN	0.051 $\pm$ 0.010	0.528 $\pm$ 0.078	170 $\pm$ 14	4756 $\pm$ 605	16.8 $\pm$ 1.0	3601 $\pm$ 44
	ED	0.352 $\pm$ 0.029	0.442 $\pm$ 0.026	270 $\pm$ 11	2873 $\pm$ 704	44.5 $\pm$ 3.1	4275 $\pm$ n.a.
<i>lhy cca1</i>	EN	<b>*0.001 <math>\pm</math> 0.001</b>	<b>*0.069 <math>\pm</math> 0.008</b>	<b>*37 <math>\pm</math> 3</b>	<b>*1931 <math>\pm</math> 429</b>	<b>*9.4 <math>\pm</math> 1.1</b>	<b>*2072 <math>\pm</math> 3</b>
	ED	0.306 $\pm$ 0.010	<b>*0.582 <math>\pm</math> 0.012</b>	261 $\pm$ 14	2407 $\pm$ 249	45.4 $\pm$ 1.4	3577 $\pm$ 287
13 days old							
Ws2	EN	0.116 $\pm$ 0.008	0.603 $\pm$ 0.041	149 $\pm$ 8	14474 $\pm$ 540	21.7 $\pm$ 0.4	n.a. $\pm$ n.a.
	ED	0.544 $\pm$ 0.006	0.773 $\pm$ 0.041	432 $\pm$ 4	12866 $\pm$ 1134	42.4 $\pm$ 1.0	n.a. $\pm$ n.a.
<i>elf3</i>	EN	0.153 $\pm$ 0.045	0.739 $\pm$ 0.043	195 $\pm$ 23	19259 $\pm$ 3946	25.6 $\pm$ 5.4	n.a. $\pm$ n.a.
	ED	<b>*0.667 <math>\pm</math> 0.026</b>	0.589 $\pm$ 0.005	242 $\pm$ 22	10224 $\pm$ 238	30.6 $\pm$ 1.0	n.a. $\pm$ n.a.



**Table 2.** Rates of starch degradation during a normal night and after a sudden early dusk in *prp7 prp9*, *toc1*, *lhy cca1*, and *elf3* clock mutants and their corresponding wild types. The rate of starch degradation during the night was estimated by linear regression against starch content between ZT12 and ZT24. The difference between the control (normal night) and early dusk was tested for significance using two-way-ANOVA (*p-values*: \*\*\* < 0.001, \*\* < 0.01, \* < 0.05). The original data are shown in Supplemental Fig. S12

	Rate of starch degradation ( $\mu\text{mol}\cdot\text{g}^{-1}\text{FW}\cdot\text{h}^{-1}$ )						
	Col-0	<i>prp7 prp9</i>	<i>toc1</i>	Ws-2 (21d.)	<i>lhy cca1</i>	Ws-2 (13d.)	<i>elf3</i>
Normal night	4.52 $\pm$ 0.32	4.08 $\pm$ 0.37	3.77 $\pm$ 0.46	2.72 $\pm$ 0.09	2.74 $\pm$ 0.11	6.47 $\pm$ 0.35	4.68 $\pm$ 0.37
Early dusk	*** 2.71 $\pm$ 0.16	* 2.90 $\pm$ 0.33	* 2.72 $\pm$ 0.21	*** 1.83 $\pm$ 0.05	*** 1.85 $\pm$ 0.06	*** 3.72 $\pm$ 0.12	*** 2.75 $\pm$ 0.18

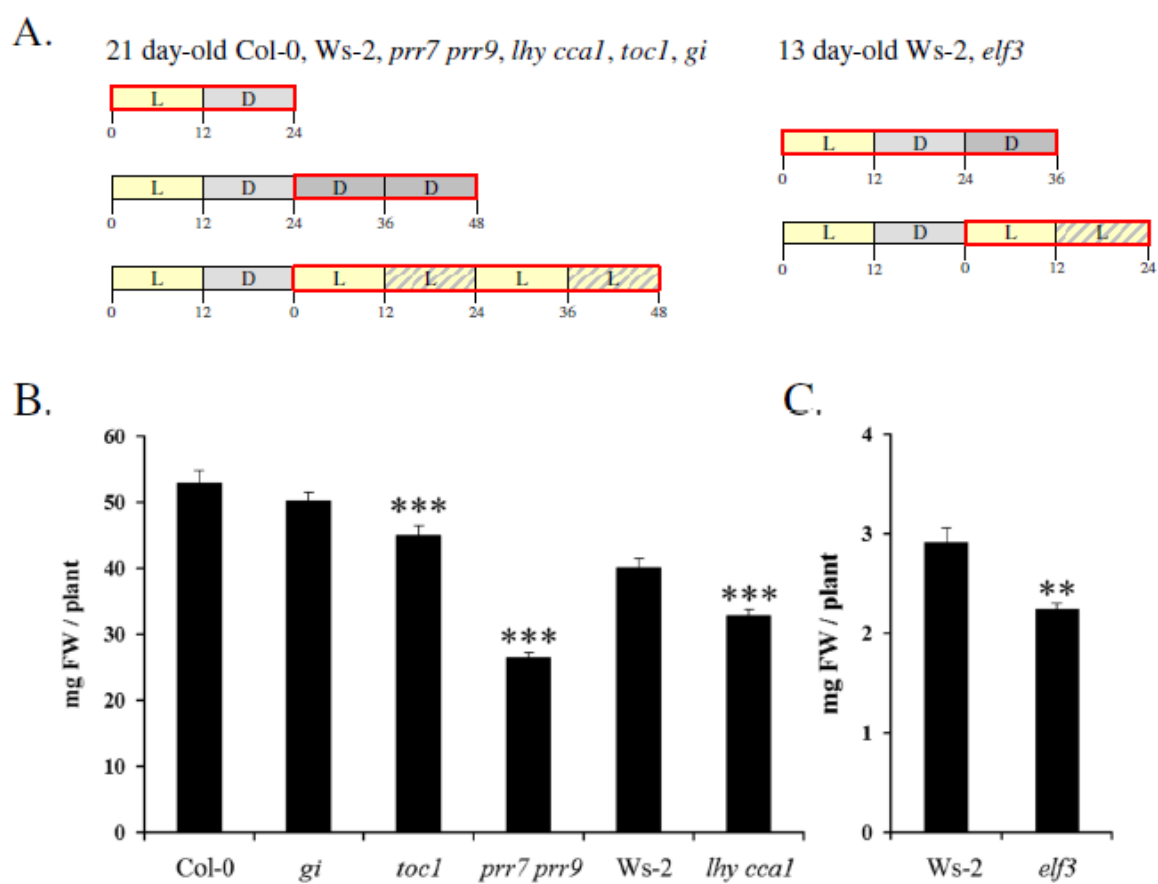


**Figure 1.** Experimental design and rosette biomass. Plants were grown in a 12 h light / 12 h dark cycle. (A) Overview of experiments. Yellow, light grey, dark grey and hatched yellow-grey shading indicate light period, night, extended night and subjective night, respectively. Subjective night denotes the interval on the 24 h cycle that had previously been night-time, i.e., darkness. Red boxes indicate the time intervals during which samples were harvested. Col-0, *Ws-2*, *gi*, *toc1*, *prp7 prp9* and *lhy cca1* were grown in a 12 h photoperiod for 21 days in three separate experiments, and harvested at 2 h intervals during a 24 h light-dark (LD) cycle, or during 24 h of extended darkness (DD), or after transfer to continuous light for 48 h (LLLL). Two samples were collected per time point (5-10 plants per sample). *Ws-2* and *elf3* were grown in a 12 h photoperiod for 13 days and then harvested at 2 h intervals during a light-dark cycle (LD) and after extension of night for another 12 h of darkness (D), or after extension of the light treatment for a further 12 h (LL). Three-four samples were collected per time point (20-50 plants per sample). This plant material was used for measurement of biomass and time-resolved analyses of protein, Chla, and Chlb (Supplemental Fig. S1), metabolites (Figs 3-5, Supplemental Figs S3-S4, S6-S7) and clock transcripts (Supplemental Figs S9-S10). (B, C) Rosette FW, calculated as the mean  $\pm$  S.E. of all 48 of the above

Accepted Article

samples for 21 day-old Col-0, Ws-2, *gi*, *toc1*, *prp7 prp9* and *lhy cca1*, and 5 samples harvested separately at ZT6 for 13 day-old Ws-2 and *elf3*. Significance was tested using Student's t-test ( $p$ -value \* < 0.05; \*\* < 0.01; \*\*\* < 0.001).

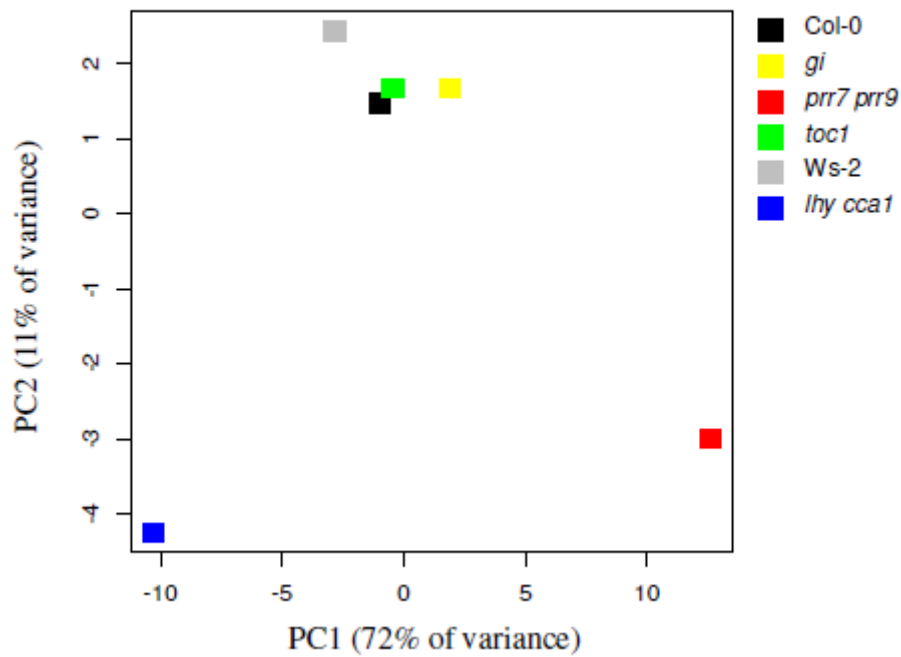


**Figure 2.** Principal Component (PC) analysis of the metabolite profile of wild type plants and clock mutants during a light dark cycle. The data are from the light-dark (LD) data series of Fig. 1. Data from 21 day-old plants. Col-0 (black), Ws-2 (21 day-old, dark grey), and a set of clock mutants, *gi* (yellow), *toc1* (green), *prp7 prp9* (red), and *lhy cca1* (blue). Additional PC analyses performed on the light-dark (LD) data series for 21 day-old Col-0 and Ws-2 wild-types, and *lhy cca1*, *prp7 prp9*, *gi* and *toc1* combined with 13 day-old Ws-2 and *elf3*, and on the second 24 hours of the continuous light data series for 21 day-old Col-0, Ws-2, *lhy cca1*, *prp7 prp9*, *toc1* and *gi* (the second cycle LL cycle of LLLL) are provided in Supplemental Fig. S2.

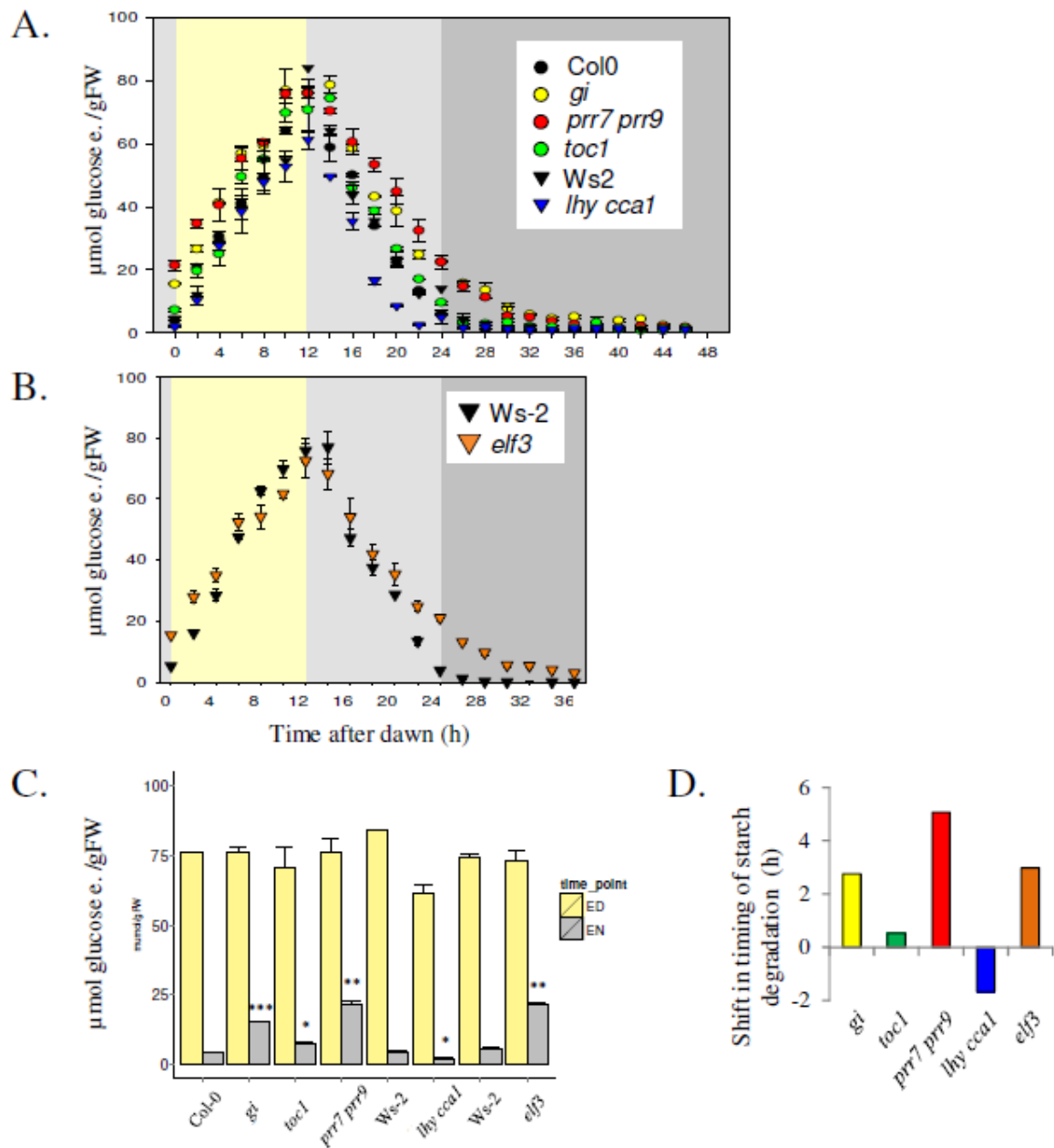


**Figure 3.** Diel changes of starch. (A) Col-0 and *Ws-2* wild-types, *lhy cca1*, *prp7 prp9*, *toc1* and *gi*. (B) *Ws-2* and *elf3*. Plants were grown in a 12 h light 12 h dark cycle and rosettes were harvested at 2 h intervals, starting at dawn for a complete light-dark cycle, and, after extension of the night for a further 24 h for 21 day old plants (LD and DD - Panel A) or for a complete light-dark cycle and, after extension of the night for 12 h for 13 day old plants (LDD - Panel B). At each time point, duplicate samples (each with 5-10 pooled rosettes) were harvested for 21 days-old plants and triplicate or quadruplicate samples (each with 20-50 rosettes) for 13 day-old plants. The results are given as mean  $\pm$  S.E. ( $n = 2$  or 3-4, respectively for the 21 or 13 day-old plants). (C) Starch content at dawn (grey) and dusk

(yellow) summarized across all genotypes (mean  $\pm$  S.E, tested using Student's t-test,  $p$ -value: \*  $< 0.05$ ; \*\*  $< 0.01$ ; \*\*\*  $< 0.001$ ). (D) Estimated shift of the time at which the rate of starch degradation during the night would lead to total exhaustion of starch in clock mutants relative to appropriate wild types (St0). The rate of starch degradation during the night was estimated using a linear regression against starch content between ZT12 and ZT24, except for *lhy cca1* where it was estimated from between ZT12 and ZT22. This rate was extrapolated to the x-axis to estimate the time at which it would lead to total depletion of starch (for details see Supplemental Table S1). The original data are in Supplemental Data files S1 and S2.



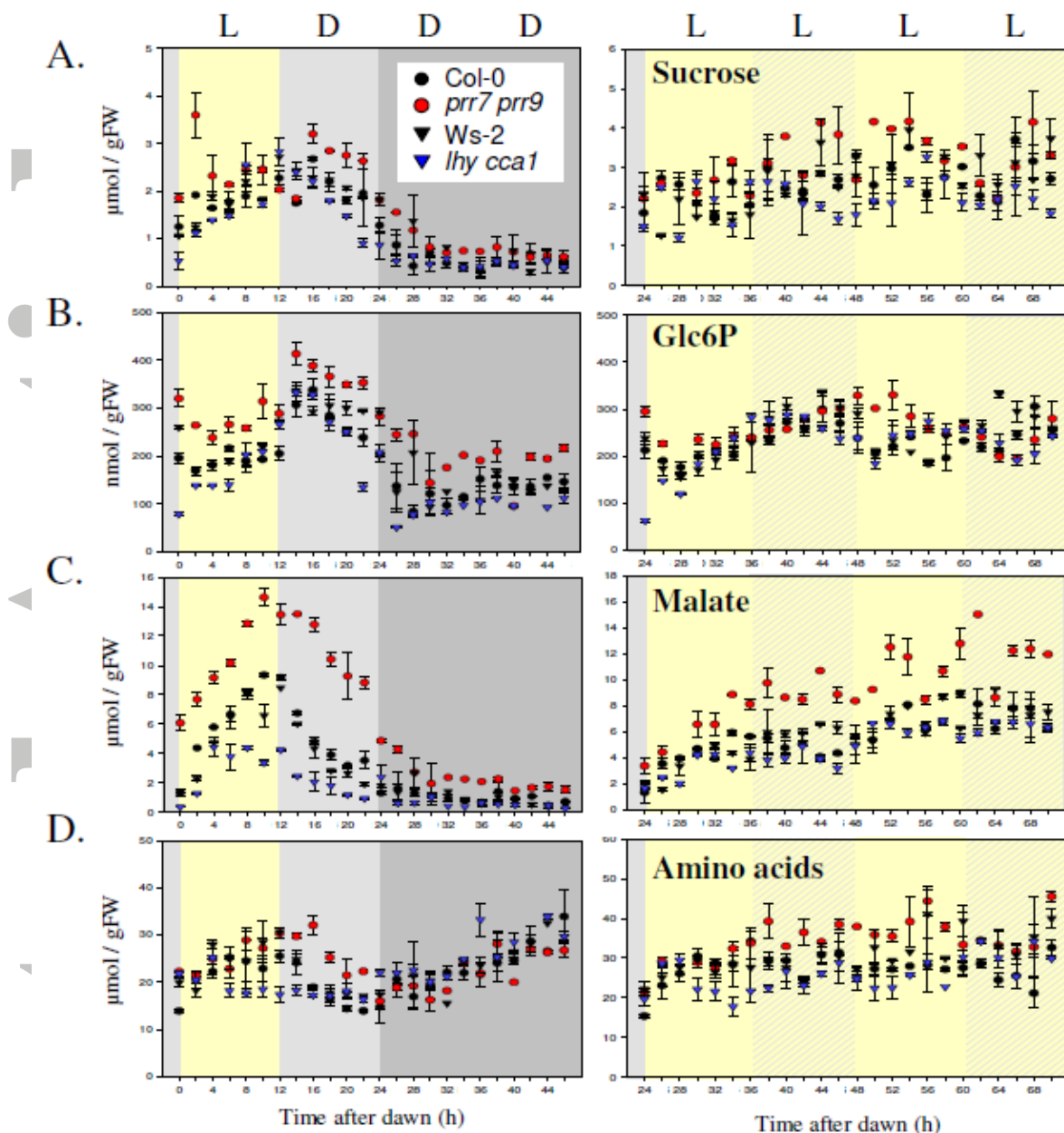


**Figure 4.** Diel changes of sugars, malate and total amino acids in Col-0, Ws-2, *lhy cca1* and *prp7 prp9*. The data are for the same experiments as those shown in Figs 1-3. The left and right subpanels show responses in a light dark cycle (LD) followed by 24 h darkness (DD), and after transfer to continuous light (LLLL), respectively. (A) Sucrose, (B) glucose 6-phosphate, (C) malate, (D) total amino acids. The results are given as mean  $\pm$  S.E. ( $n = 2$ ). Full plots of all genotypes and plots of further metabolites are provided in Supplemental Fig. S3. The original data are given in Supplemental Data files S1.

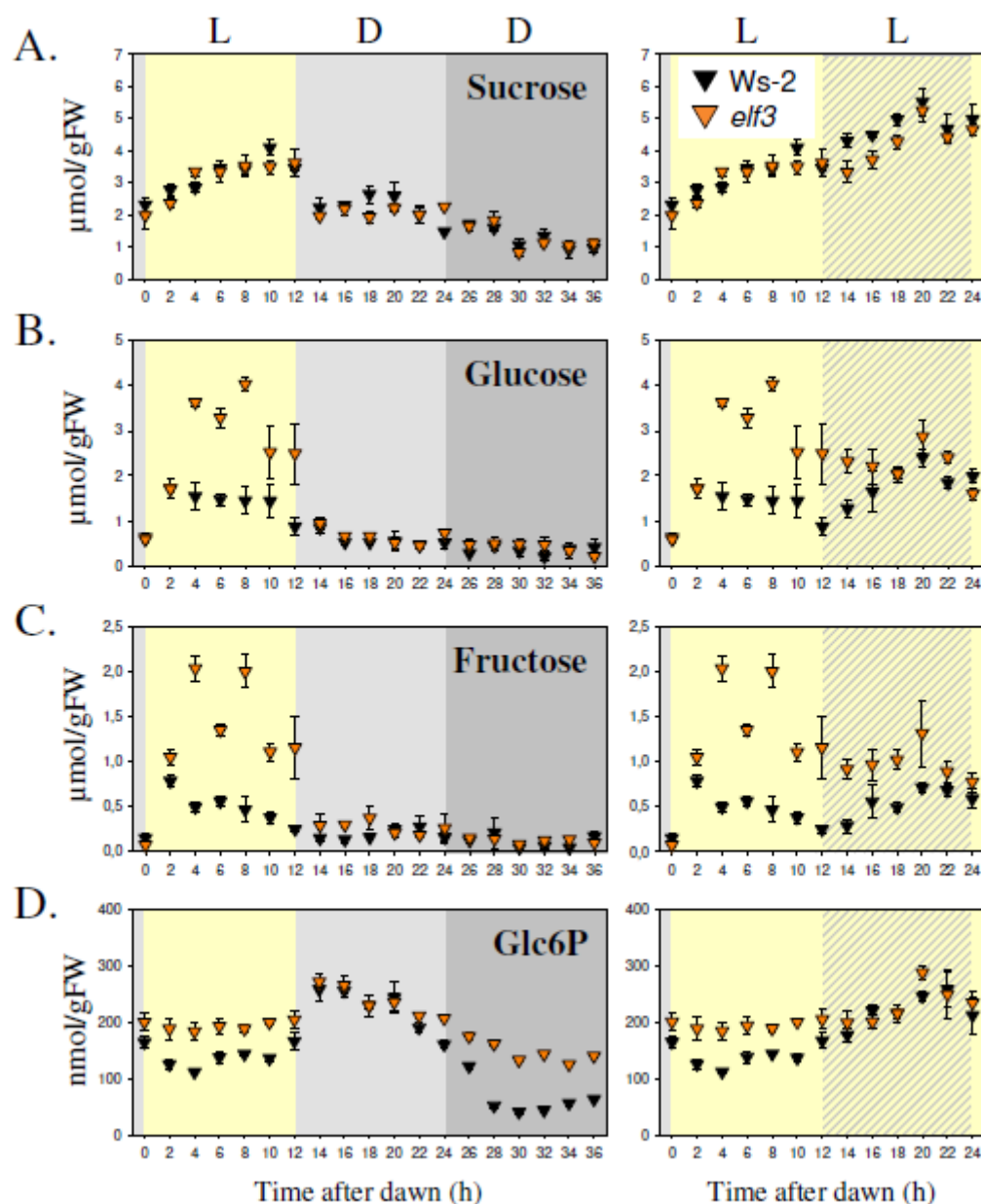


**Figure 5.** Diurnal changes of sugars in *Ws-2* and *elf3*. The data are for the same experiments as those shown in Figs 1-3. The left and right hand subpanels show responses in a light-dark cycle followed by 12 h of darkness (LDD and in 24 h of continuous light (LL), respectively. (A) Sucrose, (B) glucose (C) fructose, (D) glucose 6-phosphate. The results are given as mean  $\pm$  S.E. ( $n = 3-4$ ). Plots of further metabolites and a replicate experiment are provided in Supplemental Fig. S4. The original data are given in Supplemental Data file S2.

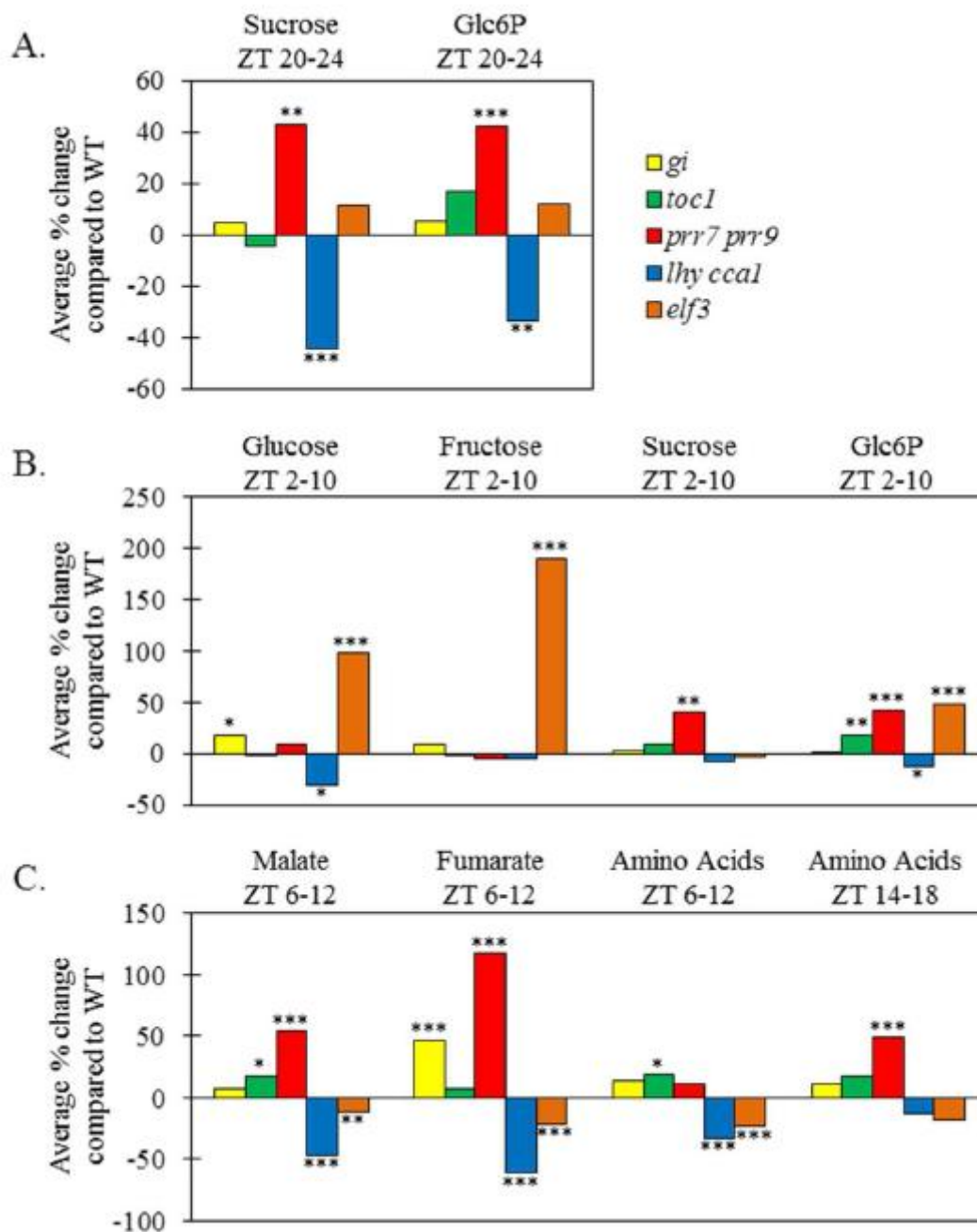


**Figure 6.** Quantification of the impact of clock components on sugars, organic acid and amino acid metabolism during selected intervals in the diurnal cycle. (A) Sucrose and Glc6P at ZT20-24. (B) Levels of soluble sugars in clock mutants relative to the corresponding wild type plants in the light period between ZT2-ZT10. (C) Levels of organic acids and amino acids in clock mutants relative to appropriate wild type in the later part of the light period (ZT6-ZT12) and levels of total amino acids at the beginning of the night (ZT14-ZT18). The comparisons were 21 day-old *toc1*, *gi* and *prr7 prr9* against 21 day-old Col-0 wild-type, 21 day-old *lhy cca1* against 21 day-old Ws-2 wild-type, and 13 day-old *elf3* against 13 day-old Ws-2. The diagram shows the value in a mutant as a percentage of the value in the

Accepted Article

corresponding wild-type, averaged across all time points in the interval. Significance was tested using ANOVA on the individual mutant and wild-type values in all samples in the time interval (\*\*\* < 0.001, \*\* < 0.01, \* < 0.05; n = 6 for ZT20-24, 10 for ZT2-10, 8 for ZT6-12 or 6 for ZT14-18).

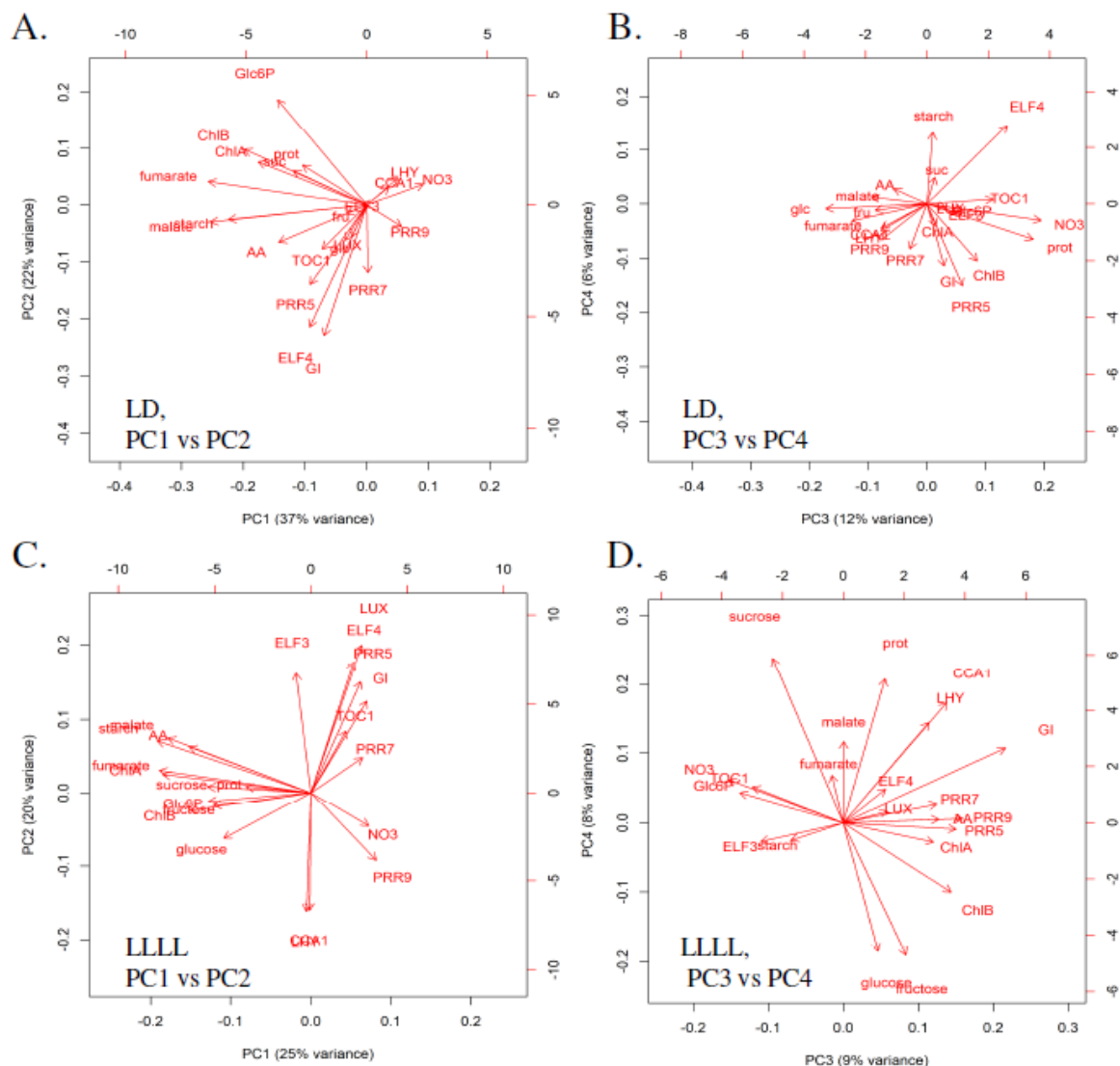


**Figure 7.** Biplot representing Principal Component (PC) analysis performed on Z-scored values of transcript and metabolic data in 21 day-old Col-0, Ws-2, *gi*, *toc1*, *prp7 prp9* and *lhy cca1*. Vectors represent the loading of each variable on the principal components (A, B) for the light-dark (LD) data series and (C, D) the second 24 h of the continuous light (second LL of LLLL) data series. Panels (A, C) show PC1 and PC2, and panels (B, D) show PC3 and PC4. The percentage of the total variance explained by each PC is given on the axis legend. Metabolites: starch, sucrose, glucose, fructose, Glc6P, total amino acids, malate, fumarate, nitrate, protein, Chla, Chlb (see original data in Supplemental Data File S1). Transcripts: *LHY*, *CCA1*, *PRR9*, *PRR7*, *PRR5*, *TOC1*, *GI*, *ELF3*, *ELF4*, *LUX* from Flis *et al.* (2015), see plots in Supplemental Figs S9 and S10.

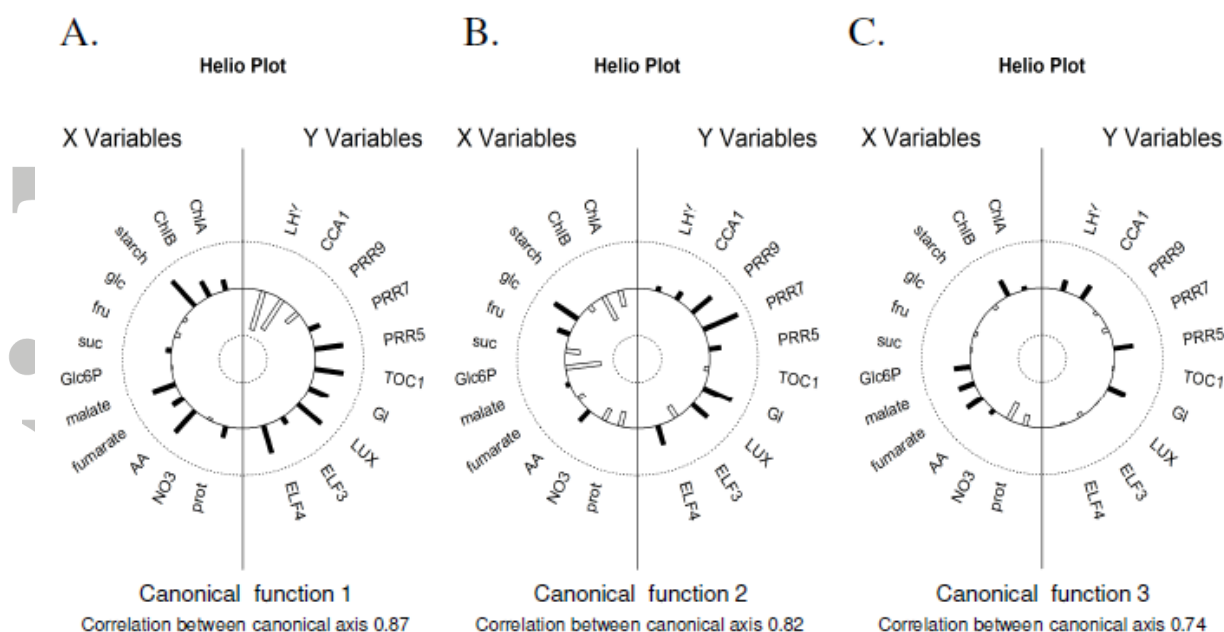


**Figure 8.** Helio plot representing results of Canonical Correlation (CC) analysis performed on Z-scored values of transcript and metabolic data collected in the light –dark (LD) cycle at 2 h intervals in 21 day-old Col-0, Ws-2, *gi*, *toc1*, *prrr7 prrr9* and *lhy cca1*. This analysis searches for a multivariate axis through one dataset (Canonical Variate X; here, metabolite data) and a multivariate axis through a second dataset (Canonical Variate Y; here, transcript data) such that the two axes are maximally correlated. The pair of axes is termed a canonical function. Following detection of the first canonical function, further correlated pairs of axes are searched for, subject to them being uncorrelated with the previous pairs of axes. The plot shows the correlations (loadings) of each individual variable with the X (metabolites) or Y (transcripts) canonical variate. Black bars and white bars distinguish between positive and negative loading, respectively, and the length of the bar represents the strength of the loading (the higher the bar, the stronger the loading). Panels A, B and C show results for 1<sup>st</sup>, 2<sup>nd</sup> and 3<sup>rd</sup> canonical correlation respectively.



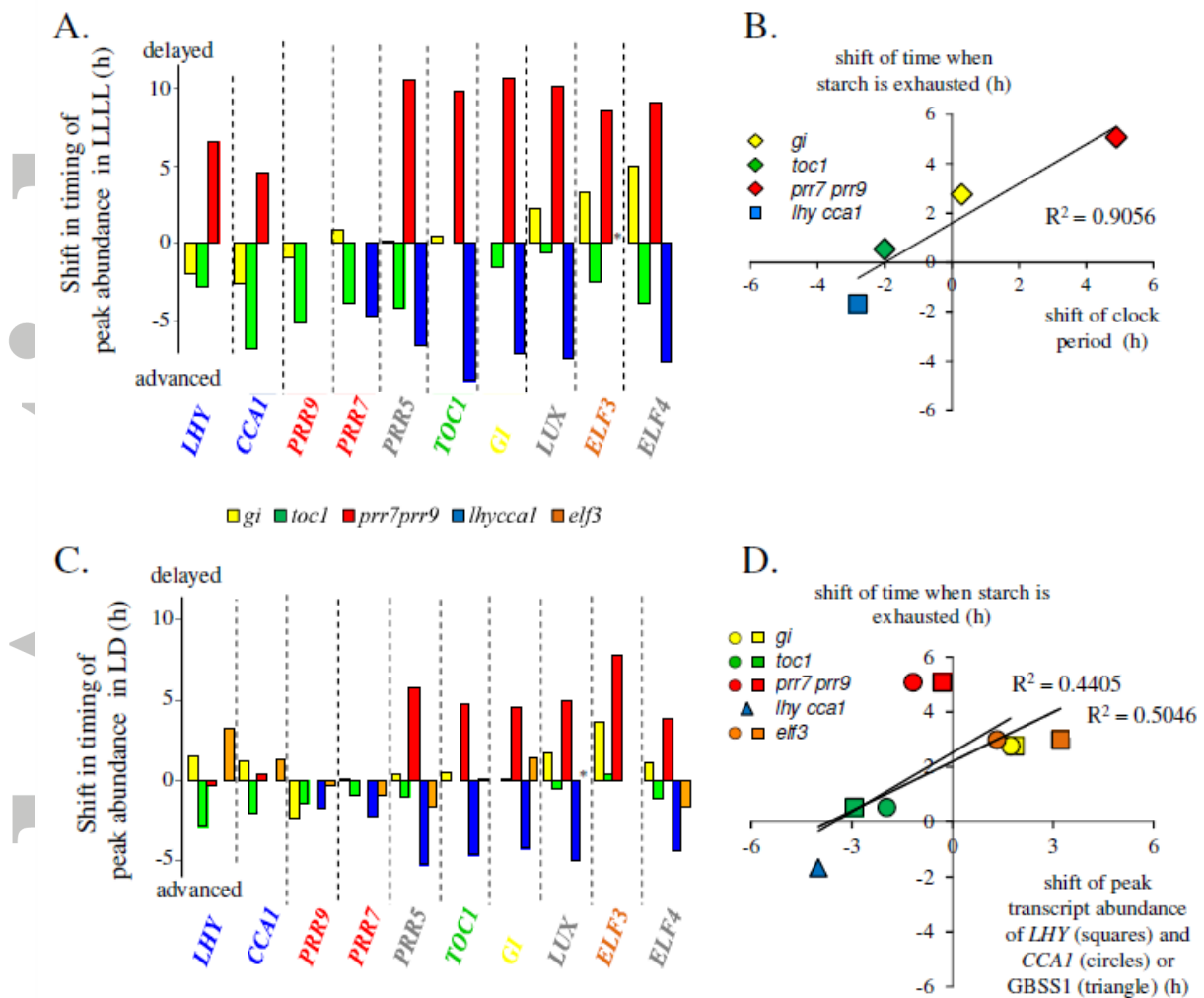


**Figure 9.** Relation between the timing of starch degradation and the timing of core clock gene expression. (A) Shift in the timing of peak transcript abundance in LLLL in clock mutants relative to appropriate wild type. (B) Comparison of the shift in clock period duration in LLLL and the shift in the timing of starch degradation, St0 (see Fig. 3D for the calculation of St0). (C) Shift in the timing of peak transcript abundance in a LD cycle in clock mutants relative to appropriate wild type. (D) Comparison of the shift in the time at which the clock anticipates dawn in an LD cycle and the shift in the timing of starch degradation, St0. The time at which the clock anticipates dawn was defined by the peak transcript abundance for the *LHY* (squares) and *CCA1* (circle) transcripts, except for the *lhy cca1* mutant where an advance of 4 h was estimated based on the known response of *GBSSI* (triangle, Graf *et al.* 2010)) and the advance of other clock gene peaks (see panel C). The regressions are shown for *GBSSI* together with for *LHY* or *CCA1* separately. In panels A-D, the shift in timing was calculated by comparing the values in a mutant with that in the corresponding wild-type treatment (21 day-old Col-0 for *toc1*, *gi* and *prp7 prp9*, 21 day-old

Ws-2 for *lhy cca1* and 13 day-old Ws-2 for *elf3*). (E) Changes in *CCA1* transcript abundance in a LD cycle in Col-0, *gi*, *toc1* and *prp7 prp9*. (F-G) Timing and amplitude of core clock peak transcript abundance in Col-0 and *prp7 prp9*.

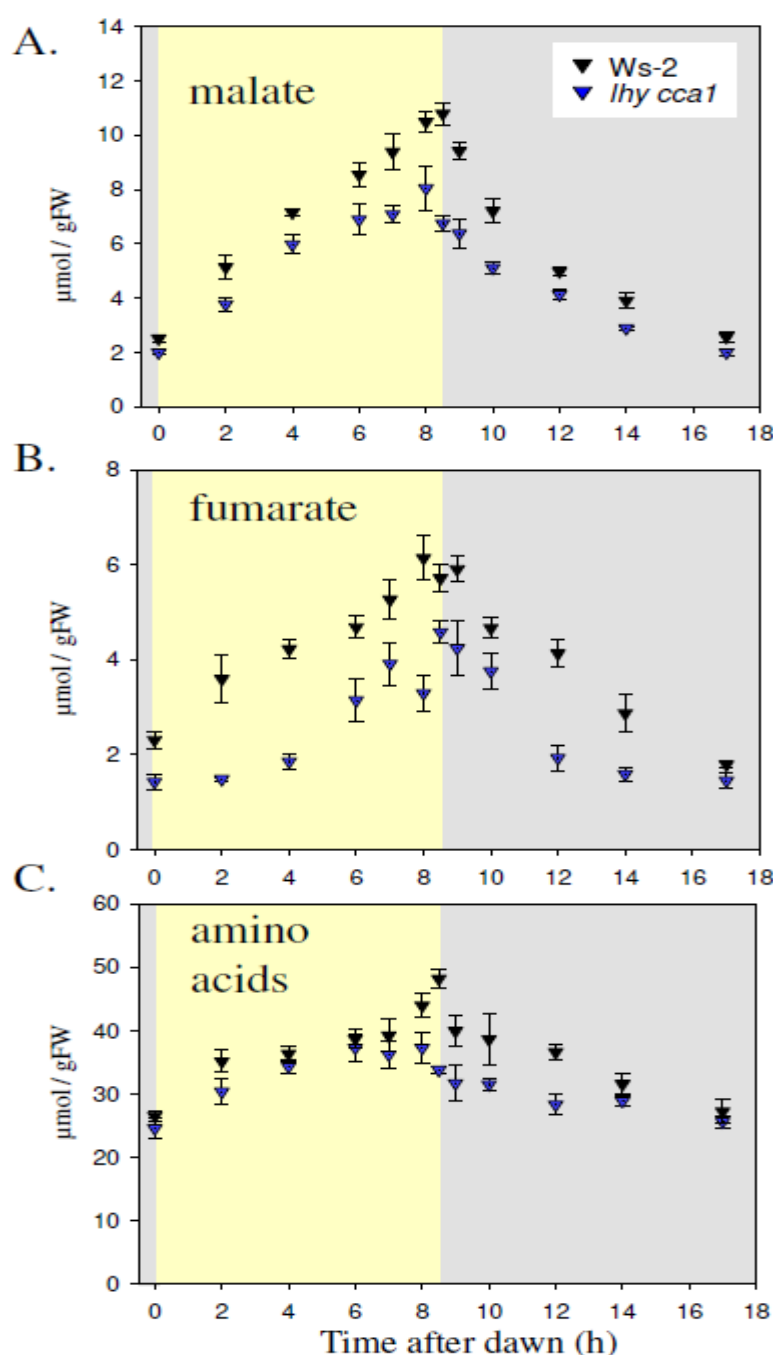


**Figure 10.** Malate, fumarate and total amino acids in wild-type Ws-2 and *lhy cca1* grown in a T-17 cycle. The *lhy cca1* mutant and Ws-2 were grown in a 8.5 h light / 8.5 h dark cycle and were harvested 21 days after sowing at 2 h intervals during a diurnal cycle (with denser harvesting around dusk). (A) Malate, (B) fumarate, (C) total amino acids. The results are the mean  $\pm$  S.E. (n = 4). Plots of further metabolites are provided in Supplemental Fig. S14. The original data are provided in Supplemental Data File S5.

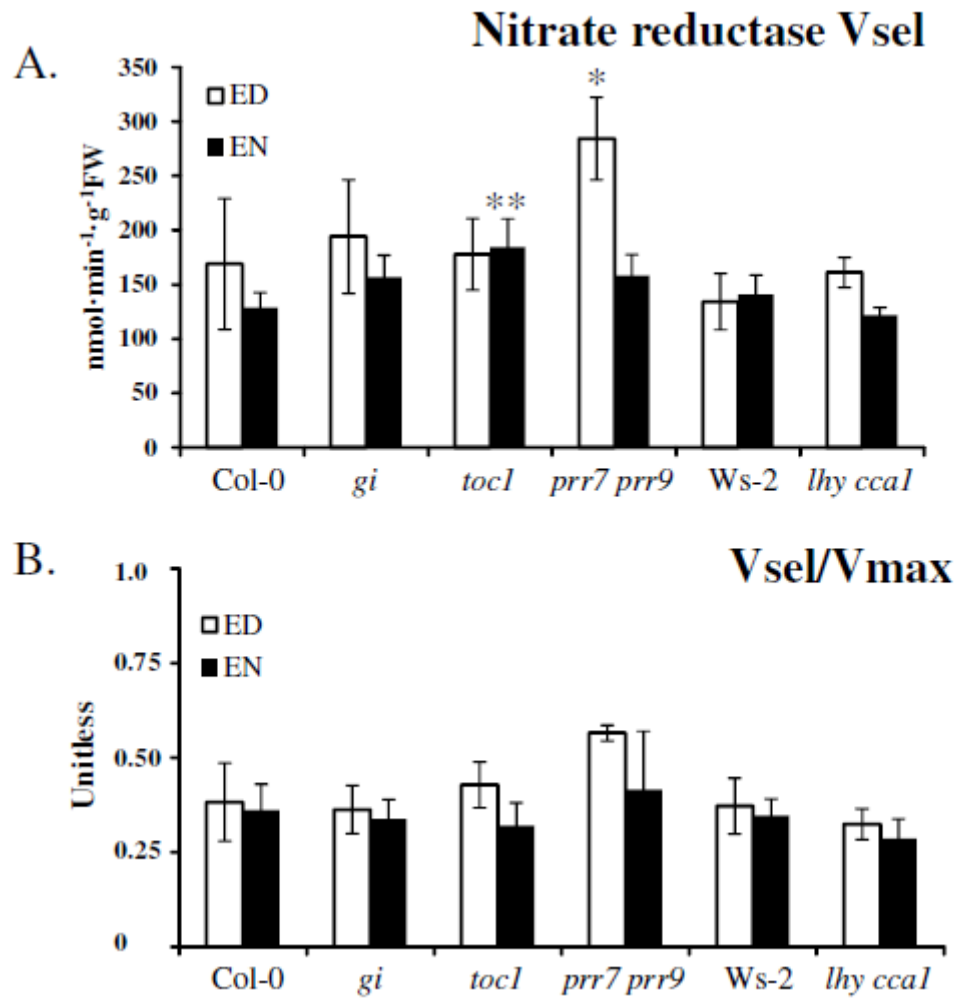


**Figure 11.** Nitrate reductase activity in Col-0 and Ws-2 wild-types, *tocl*, *gi*, *lhy ccal* and *prr7 prr9*. Nitrate reductase activity was determined in the absence of magnesium (Vmax) and in the presence of magnesium to allow binding of inhibitory 14-3-3 protein to the phosphorylated form of nitrate reductase (selective activity assay, Vsel). Activity was assayed in samples collected just before illumination (dark bars) and at the end of the light period just before darkening (white bars). (A) Selective activity (Vsel). (B) The ratio of Vsel to Vmax activity, providing a measure of post-translational activation of nitrate reductase. The results are the mean  $\pm$  S.E. ( $n = 2$ ). Significance was tested using Student's t-test, p-value \*  $< 0.05$ ; \*\*  $< 0.01$ ; \*\*\*  $< 0.001$ ).

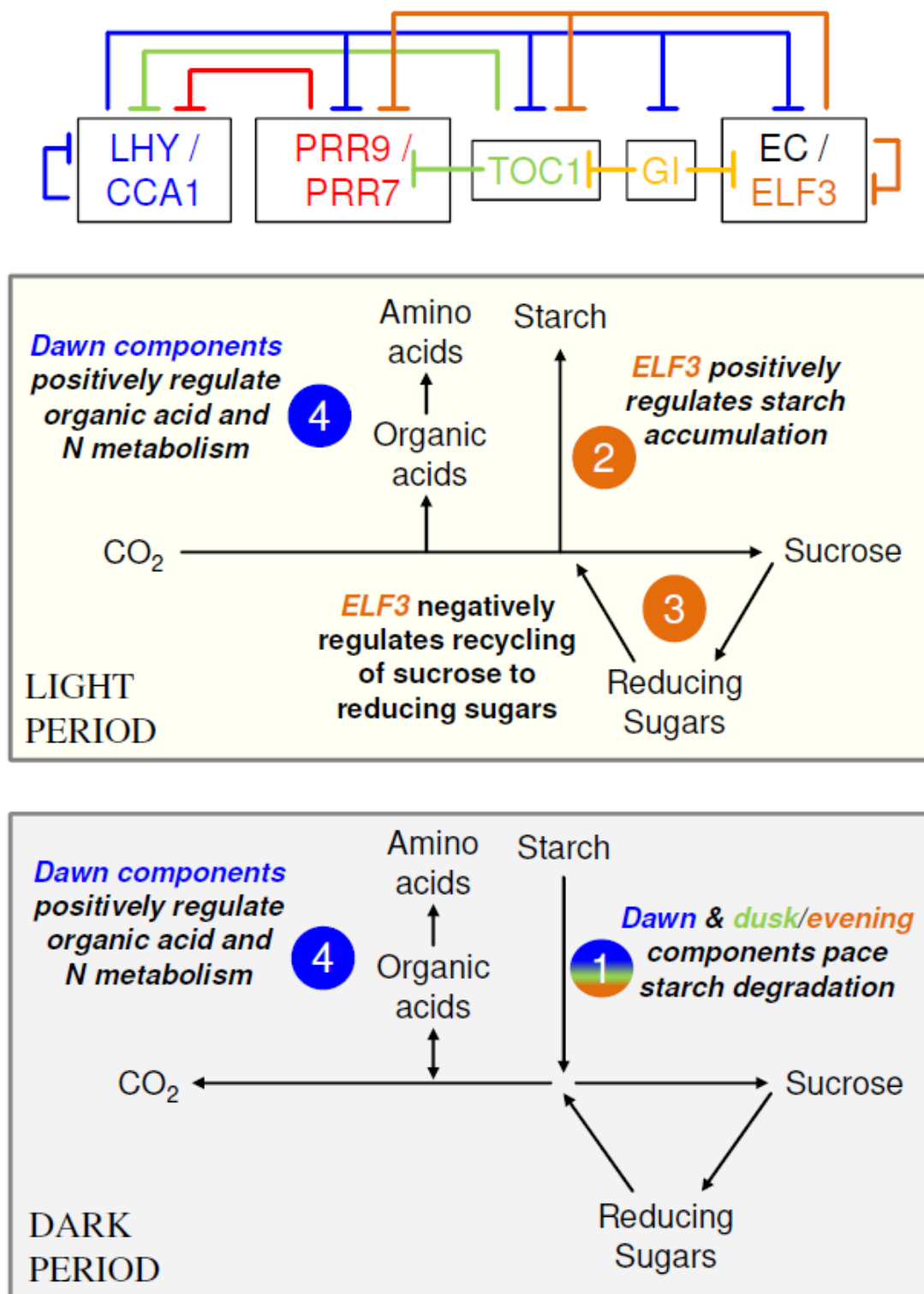


**Figure 12.** Schematic summary of clock outputs that regulate central carbon metabolism in Arabidopsis leaves. Main metabolic fluxes of C are shown for the light (pale yellow box) and darkness (pale grey box). The clock is depicted using circadian clock component according to the model in Pokhilko *et al.*, (2012), with dawn (*LHY*, *CCA1*), morning (*PRR9*, *PRR7*), dusk

(*PRR5*, *TOC1*, *GI*) and evening (*LUX*, *ELF4*, *ELF3*) components. Four main outputs are indicated: (1) An output regulating the rate of starch accumulation in the light period, in which *ELF3* may play a major role. (2) An output in which *ELF3* regulates the levels of reducing sugars in the first part of the 24 h cycle. This may serve to regulate the net rate of sucrose production and, hence starch accumulation, and also to support expansion growth. (3) An integrated output from dawn components and dusk/evening components that regulates the rate of starch degradation at night such that starch is almost but not completely exhausted at dawn, thus ensuring that the plant does not become C-starved at the end of the night. This or a related output may also, by regulating when starch degradation occurs in the light, be responsible for the circadian oscillation in Glc6P (not shown on this figure). (4) An output in which the dawn components play a major role regulates organic acid and N metabolism and is important in establishing and maintaining pools of organic acids, as well as amino acid reserves to support protein synthesis in the coming night. For more details see the text. Action of these outputs in the light period and the night is shown in different sub-panels.